Neurobiology of Aging 92 (2020) 43–60

Contents lists available at ScienceDirect

Neurobiology of Aging

journal homepage: www.elsevier.com/locate/neuaging

The vulnerability of motor and frontal cortex-dependent behaviors in mice expressing ALS-linked mutation in TDP-43

Peiyan Wong[a], Wan Yun Ho[b], Yi-Chun Yen[b,1], Emma Sanford[b], Shuo-Chien Ling[b,c,d,*]

[a] Department of Pharmacology, National University of Singapore, Singapore
[b] Department of Physiology, National University of Singapore, Singapore
[c] Department of Neurobiology/Ageing Programme, National University of Singapore, Singapore
[d] Program in Neuroscience and Behavior Disorders, Duke-NUS Medical School, Singapore

ARTICLE INFO

Article history:
Received 30 September 2019
Received in revised form 18 March 2020
Accepted 29 March 2020
Available online 9 April 2020

Keywords:
Amyotrophic lateral sclerosis
Frontotemporal dementia
TDP-43
Cognition
Frontal cortex
Hippocampus

ABSTRACT

TDP-43 aggregates are the defining pathological hallmark for amyotrophic lateral sclerosis (ALS) and frontotemporal dementia (FTD). Strikingly, these TDP-43 proteinopathies are also found in other neurodegenerative diseases, including Alzheimer's disease and are prevalent in the brains of old-aged humans. Furthermore, disease-causal mutations in TDP-43 have been identified for ALS and FTD. Collectively, the evidence indicates that TDP-43 dysfunctions lead to motor and cognitive deficits. To determine whether the mouse line expressing an ALS-linked mutation in TDP-43 (Q331K) can be used to study ALS-FTD spectrum disorders, we performed a systematic and longitudinal behavioral assessment that covered motor and cognitive functions. Deficits in motor and cognitive abilities were observed as early as 3 months of age and persisted through to 12 months of age. Within the cognitive modalities, the hippocampus-mediated spatial learning and memory, and contextual fear conditioning, were normal; whereas the frontal cortex-mediated working memory and cognitive flexibility were impaired. Biochemically, the human TDP-43 transgene downregulates endogenous mouse TDP-43 mRNA and protein, resulting in human TDP-43 protein that is comparable with the physiological level in cerebral cortex and hippocampus. Furthermore, Q331K TDP-43 is largely retained at the nucleus without apparent aggregates. Taken together, our data suggest that motor and frontal cortex may be more vulnerable to disease-linked mutation in TDP-43 and, this mouse model may be used to assess ALS-FTD–related spectrum diseases and the molecular underpinnings associated with the phenotypes.

1. Introduction

Due to the pivotal discovery that identified abnormal TDP-43 aggregates as the defining pathological hallmarks for most patients with amyotrophic lateral sclerosis (ALS) and a subgroup of patients with frontotemporal dementia (FTD) (Arai et al., 2006; Neumann et al., 2006), these TDP-43 aggregates, also known as TDP-43 proteinopathies, have also been found in patients with Alzheimer's disease (AD) (Josephs et al., 2014; Nag et al., 2018) and hippocampal sclerosis (HS, a condition with very similar symptoms to AD) (Aoki et al., 2015; Nag et al., 2015). Furthermore, abnormal TDP-43 aggregates are prevalent in the brains of old-aged humans (McAleese et al., 2017; Uchino et al., 2015). Intriguingly, a new disease entity, coined as limbic-predominant age-related TDP-43 encephalopathy, also has a TDP-43 pathology within medial temporal lobe structures in patients older than 80 years. These patients with limbic-predominant age-related TDP-43 encephalopathy have cognitive impairment mimicking AD (Nelson et al., 2019). Given that the severity and symptoms of each disease typically correlate with the TDP-43 pathologies within the affected regions of the central nervous system (Brettschneider et al., 2015), evidence indicates that TDP-43 is critical in maintaining CNS functions, and TDP-43 dysfunctions can result in motor and cognitive impairments.

To date, more than 50 mutations in TDP-43 have been identified to cause and/or link with ALS and FTD (Lattante et al., 2013; Ling, 2018; Ling et al., 2013). The gene-pathology relationship is reminiscent of other major neurodegenerative diseases, such as AD and Parkinson's disease, whereby the pathological hallmarks detected in the CNS are, in part, a consequence of the products encoded by

* Corresponding author at: Department of Physiology, Yong Loo Lin School of Medicine, National University of Singapore, Tahir Foundation Building, MD1, 16-03-H 12 Science Drive 2, Singapore 117549. Tel.: +65 6601 3645; +65 6516 3668; fax: +65 6778 8161.
E-mail address: phsling@nus.edu.sg (S.-C. Ling).
[1] Present address: Department of Life Science, Tunghai University, Taichung, Taiwan.

0197-4580/
https://doi.org/10.1016/j.neurobiolaging.2020.03.019

the mutant genes in the rare familial forms of the disease (Bertram and Tanzi, 2005). As symptoms are indistinguishable between the inherited, which is caused by genetic mutations, and sporadic forms of neurodegenerative diseases, model systems expressing disease-causal mutations are often used to investigate the underlying pathogenic mechanisms. This study and other research have shown that mice expressing ALS-linked TDP-43 mutations, such as A315T, Q331K, and M337V, develop ALS/FTD-like pathology and symptoms (Arnold et al., 2013; Wegorzewska et al., 2009). More recently, knock-in mice expressing Q331K (mutation associated with sporadic ALS) and M337V (mutation causal for familial ALS) were developed. TDP-43 M337V knock-in mice developed a mutant dose-dependent motor phenotype (Ebstein et al., 2019). By contrast, TDP-43 Q331K knock-in mice developed behavioral abnormalities mimicking aspects of FTD-like symptoms but present with no motor phenotypes (White et al., 2018). Thus, it remains to be determined whether mice expressing ALS-linked mutations in TDP-43 can develop both motor and cognitive phenotypes.

In humans, the prefrontal cortex, which is interconnected with many other cortical regions, is involved in executive functions, including working or short-term memory (STM), control of attention, and cognitive flexibility (Fuster, 2001; Kim et al., 2011), whereas the hippocampus is important for long-term declarative memory and the consolidation and retrieval of recognition and spatial memory (Ben-Yakov et al., 2015; Burgess et al., 2002; Eichenbaum, 2004). Given that (1) the CNS is organized into functional domains, (2) impaired executive function, declarative memory, and motor coordination are attributed to TDP-43 proteinopathy in the respective affected brain regions, such as the frontal and temporal lobes and the motor cortex (Amador-Ortiz et al., 2007; Brettschneider et al., 2012; Rohrer et al., 2010; Tsermentseli et al., 2012), and (3) the functional domains within CNS are conserved between rodents and human (Ben-Yakov et al., 2015; Foster et al., 2012; Franklin and Chudasama, 2012), we aimed to provide a basis for correlating phenotypes in mice with clinical presentations in humans by determining whether mice expressing ALS-linked mutation in TDP-43 (Arnold et al., 2013) can develop behavior phenotypes that mimic ALS, FTD, and/or AD spectrum disease. Furthermore, if cognitive deficits were to occur, would disease-relevant regions, such as the hippocampus or the frontal lobe, be selectively affected in this model?

To this end, we assessed the motor and cognition phenotypes in mice expressing an ALS-linked mutation (Q331K) in TDP-43 (Arnold et al., 2013) in a systematic and longitudinal fashion. These Q331K mice developed motor and cognitive deficits as early as 3 months of age and persisted through to 12 months of age. Although Q331K mice were comparable with their nontransgenic littermate controls in hippocampus-dependent tasks, they performed poorly in fontal cortex-mediated tasks, such as those that required working memory and cognitive flexibility (Boulougouris et al., 2007; McDonald and White, 1994; Rich and Shapiro, 2007; Tsutsui et al., 2016). Furthermore, Q331K transgene expresses at the normal physiological level as the endogenous mouse TDP-43 in the cerebral cortex and hippocampus without apparent aggregates. Collectively, the data suggest that the motor and frontal cortex may be more susceptible to TDP-43-mediated damages. Thus, this TDP-43 mouse model may be used to assess ALS-FTD-related spectrum diseases and the molecular underpinnings associated with the phenotypes.

2. Materials and methods

2.1. Animals

All studies were carried out under protocols approved by the Institutional Animal Care and Use Committee of the National University of Singapore and were in compliance with the Association for Assessment of Laboratory Animal Care guidelines for animal use. Q331K mice were described previously (Arnold et al., 2013) and were available via Jackson Laboratory (stock number 017933). All mice were back-crossed with C57BL/6J mice for more than 10 generations and maintained on a C57BL/6J background. Animals were housed in ventilated cages with up to 5 animals in a specific pathogen-free environment, with *ad libitum* access to food and water, on a 12-hour light/dark cycle (lights on at 0700). These Q331K mice developed lower motor neuron degeneration and motor phenotype without TDP-43 aggregates (Arnold et al., 2013). A total of 9 Q331K females, 6 Q331K males, 6 nontransgenic females, and 7 nontransgenic males were used. For genotyping, genomic DNA was isolated from tail biopsies using salt extraction methods and subjected to routine PCR methods using the following primers: TDP-43 transgene: 5′-tctgcccacttggagctagt-3′ and 5′-aggggtcaaacgatcctctc-3'.

2.2. Open field test

Locomotor activity recordings were carried out using a square open field (25 × 25 cm) in a plexiglass cage equipped with video camera recording. The animals were introduced into the locomotor cage and allowed to explore freely for an hour. The distances traveled by the animals were recorded and analyzed by the Topscan software (Cleversys Inc, Reston, V, USA).

2.3. Balance beam test

Beams that were 80 mm in length, with 2 different widths (6 mm and 12 mm), were used in the balance beam test for motor coordination. A bright light was used as an aversive stimulus at the start platform and an escape box (20 × 20 × 20 cm) was placed at the end of the beam. The animals were trained for 3 consecutive trials on each beam for 4 consecutive days, and then tested on the fifth day. The time taken to traverse the beam was recorded for each trial. The maximum time cutoff was 60 seconds.

2.4. Rotarod test

The animals were placed on the rotarod apparatus (Ugo Basile, Italy) that linearly accelerated from 4 rpm to 40 rpm at a rate of 0.1 rpm/s. The maximum cutoff time was 600 seconds. The animals were tested in 4 trials over 5 consecutive days, with a 15-minute rest period between trials. The animals' latencies to fall were recorded.

2.5. Y-maze spontaneous alternation test

The animals were placed in the center of a Y-shaped maze with 3 arms at a 120° angle from each other, for 10 minutes. If an animal had an intact spatial working memory, it would have a reduced tendency to enter the recently visited arm. The exploration activities of the animals were recorded and analyzed by Topscan (Cleversys Inc). A spontaneous alternation was defined as 3 consecutive entries of different arms. The spontaneous alternation percentage was calculated as 100*(number of spontaneous alternations)/(total number of arm entries -2).

2.6. Novel object recognition test

The novel object recognition test for mice consisted of 2 days of exposure, one day of training, and a STM test, which took place 20 minutes after training. After that, a long-term memory (LTM) test took place 16–24 hours and a remote memory (RM) test 10–14 days after training, as described previously (Wong et al., 2015).

Interactions with the objects were video-recorded and analyzed by Topscan (Cleversys Inc) and data were presented as percentage of interaction time that was spent with the novel object. The sets of objects used were different for each of the assessed time points.

2.7. Social transmission of food preference test

The social transmission of food preference test was carried out as previously described (Wong et al., 2015). In brief, mice were placed on food restriction for 16 hours the day before testing. A demonstrator mouse was allowed to consume a familiar diet and then allowed to interact with tester mice for 20 minutes. Tester mice were then exposed to a familiar diet and a novel diet, and the consumptions of each diet were monitored. The familiar diet was made from 1% of ground oregano (McCormick & Co Inc, Hunt Valley, MD, USA) in standard mouse chow. Novel diets for STM, LTM, and RM were flavored with 1% ground thyme, marjoram, and cumin (McCormick & Co Inc, USA), respectively. STM, LTM, and RM probes were carried out 20 minutes, 16–24 hours, and 10–14 days, respectively, after exposures to the demonstrator mouse. Data were presented as the amount of familiar food consumed as a percentage of total food consumption. The sets of flavored diets used were different for each of the assessed time points.

2.8. Working memory test using the water maze

Spatial working memory was assessed in the water maze using a protocol as described in Vorhees and Williams' study (2006) with slight modifications. The test was carried out across 3 days, and the animals were given 4 trials each day. The drop location and platform location remained the same across the trials within each day. Each trial lasted a maximum of 120 seconds with a 20-second intertrial interval. On the second day, the drop location and the platform location changed so that no learning of the platform position from the previous day would be transferred. The test was video-recorded and analyzed by Ethovision XT (the Netherlands). The visual cues and water maze pools used were different for each of the assessed time points.

2.9. Hidden platform water maze—spatial acquisition test

The spatial acquisition phase of the hidden platform water maze was carried out as described previously but with some modifications (Vorhees and Williams, 2006). Mice were placed in a tank containing water that was approximately 1.2 m in diameter and the water was maintained at 24–26 °C throughout the experiment. Hidden under the water in one of the quadrants was an escape platform. The water was made murky with nontoxic poster paint (meeting European and/or USA safety standards that they were rated safe for contact and consumption). The animals were allowed 60 seconds to explore. If they could not find the platform, they were guided to the platform and were allowed to remain there for 10 seconds. The animals were then towel-dried and returned to their home cages. Twenty minutes after the training was completed on the first day, an STM probe was carried out. After which, the mice were trained for 5 further days. 16–24 hours after the last training session, an LTM probe was carried out. The maximum probe trial duration was 60 seconds. The maximum number of trials per day was 4 trials, with a 60 seconds intertrial interval. The test was recorded and analyzed by Ethovision XT (the Netherlands). The visual cues and water maze pools used were different for each of the assessed time points.

2.10. Hidden platform water maze—spatial reversal test

The spatial reversal phase of the hidden platform water maze was carried out as described previously (Vorhees and Williams, 2006) with modifications. On the next day after the LTM probe was used for the spatial acquisition paradigm, the escape platform was relocated to the opposite quadrant. Animals were then trained and probed in the same way as the spatial acquisition paradigm. The visual cues and water maze pools used were different for each of the assessed time points.

2.11. Context-dependent fear conditioning test

The animals were placed in a standard conditioning box with a floor consisting of a grid of metal bars (Cleversys Inc, Reston, VA, USA). The animals were allowed to explore the box for 2 minutes, followed by 3 foot-shocks delivered at 60-second intervals. The foot-shock consisted of a pulsating 50 Hz current with 0.5 mA current. The animals were then allowed to remain in the box for 2 more minutes before being returned to their home cages. At intervals of 20 minutes, 16–24 hours, and 10–14 days, the animals were brought back to the same chamber for 3 minutes for the STM, LTM, and RM probes, respectively. The number of freezes was recorded and analyzed by Freezescan (Cleversys Inc, Reston, VA, USA). The contextual cues used were different for each of the time points.

2.12. Statistical analysis for the behavioral tests

The R statistical program (R Foundation for Statistical Computing, Vienna, Austria) was used for data analyses. Data were expressed as means ±SEM and $p < 0.05$ was considered statistically significant. For all tests, genotype and age were between subject factors, whereas repeated test sessions were within subject factors. The normality of the residuals were assessed using the tools for building OLS regression models package and no violations of normality was found. The homogeneity of variance was assessed using the Levene's test from the car statistical package. In cases where there were no violations to assumptions of normality and homogeneity of variation, the regression models were fit using lmer() in the lmerTest statistical package (Kuznetsova et al., 2017). They were then assessed using anova() from the stats package. For instances where the assumption of homogeneity of variance was violated, which includes the data for the rotarod, balance beam, and novel object recognition behavioral tests, the resulting regression models were fit using glmer() from the from the lme4 statistical package (Bates et al., 2015). They were then assessed using Anova() in the car package. The statistical information from the regression models are reported in the respective tables that are cited in the texts. Estimated marginal means were used for post hoc tests, with the Tukey method of adjustment used when there were multiple comparisons.

2.13. RNA extraction, cDNA synthesis, qRT-PCR

Total RNAs were extracted from cerebral cortex and hippocampus using Trizol reagent (Thermo Fisher Scientific) according to manufacturer's instruction. After DNase treatment using RQ1 RNase-Free DNase (Promega), 1 μg RNA were reversely transcribed using Maxima First Strand cDNA Synthesis Kit for RT-qPCR (Thermo Fisher Scientific). All qRT-PCR reactions were performed with at least 3 biological replicates for each group and 3 technical replicates. mRNA levels were determined using Maxima SYBR Green qPCR master mix (Thermo Fisher Scientific). The forward and reverse primer sequences were validated in-house and listed below: mouse

TDP-43: forward primer, 5′-TTCAGAGCTTTTGCCTTCGT-3′, reverse primer, 5′-AGCTCCACCCCCTCTACTGT-3’; mouse GAPDH: forward primer 5′-AGGCCGGTGCTGAGTATGTCGTG-3′, reverse primer, 5′-TCGGCAGAAGGGGCGGAGAT-3’; mouse ARHGDIA: forward primer 5′-CTCGGGGCAGTTACAACATCAAGTC-3′, reverse primer, 5′-GTCGCCCTGCCCGTCTCC-3’. Expression values were normalized to 2 control genes: GAPDH and ARHGDIA mRNA and geometric means were used to calculate the relative expression values. Expression values were expressed as a percentage of the average expression of control samples and data was analyzed using Student's *t*-test.

2.14. Tissue protein extraction and immunoblotting

Total proteins were extracted from cerebral cortex and hippocampus using Trizol reagent (Thermo Fisher Scientific) after RNA were extracted according to manufacturer's instruction. Recombinant human and mouse TDP-43 were purified as described previously (Ling et al., 2010). Each sample was loaded for 12% Bis-Tris-PAGE and transferred to nitrocellulose membrane using 1× transfer buffer containing 1× Tris-Glycine (25 mM Tris base and 192 mM glycine) and 20% methanol supplemented with 0.02% SDS at 80V for 120 minutes. Membranes were blocked using 5% milk in 1× TBST (50 mM Tris, 150 mM NaCl, 0.1% Tween 20, pH 7.4) at room temperature for 1 hour. After blocking, membranes were incubated with primary antibodies at 4 °C overnight. The primary antibodies used in this study were TDP-43 (Proteintech, cat# 12,892, 1:2000) and GAPDH (Proteintech, cat# 60,004, 1:5000). Membranes were washed with 1XTBST and incubated with appropriate HRP-conjugated secondary antibodies (1:5000, Cell Signaling Technology) at room temperature for 1 hour. After washing with 1xTBST extensively, target proteins were probed using SuperSignal™ West Pico Chemiluminescent Substrate (Thermo Fisher Scientific). Images were captured with a ChemiDoc (Bio-Rad) and quantified with Image Lab software (Bio-Rad).

2.15. Immunofluorescence

Tissue preparation for immunohistochemistry was described previously (Ho et al., 2019; Wang et al., 2018). In brief, mice were anesthetized with isoflurane and perfused transcardially with phosphate-buffered saline (PBS), followed by 4% paraformaldehyde (PFA) in phosphate buffer for fixation. Brains were dissected and postfixed in 4% PFA in PBS for 2 hours. Tissues were cryopreserved in 30% sucrose for over 24 hours and embedded in Tissue-Tek before sectioning. Brains were sectioned coronally into PBS at 30 μm using a cryostat or microtome. Antigen retrieval was performed for immunofluorescence against myc. Antigen retrieval was performed via heating the tissues in citrate buffer (10 mM sodium citrate, 0.05% Tween 20, pH 6.0) at 95 °C for 15 minutes before starting the immunofluorescence protocol. For brain section staining, after 3 washes with 1×PBS, sections were treated with 10 mM glycine for 15 minutes each to remove any possible PFA remnants. The tissues were then permeabilized with 0.3% Triton X-100 in 1× PBS, and blocked in blocking serum, 5% donkey serum with 0.3% Triton X-100 in 1X PBS. Incubation with primary antibodies diluted in 1% donkey serum and 1X PBS in blocking serum were performed overnight at 4 °C. Tissues were then washed 3 times for 15 minutes in 1X PBS. Incubation of secondary antibodies conjugated with Alexa Fluor 488, 568, 643 (1:1000, Thermo Fisher Scientific) and 1 μg/mL DAPI were performed in 0.1% Triton X-100 with 1% Donkey Serum in 1× PBS for overnight at 4 °C. Tissues were washed in 0.1% Triton X-100 in 1× PBS for 3 times for 15 minutes before mounting onto slides with Prolong Gold anti-fade reagent (Thermo Fisher Scientific, P36930). The primary antibodies used in this study were TDP-43 (Proteintech, cat# 10782), myc-tag (Proteintech, cat# 16286), and lamin B (Proteintech, cat# 66095).

2.16. Image acquisition

Confocal images were acquired with a Zeiss LSM700 inverted confocal microscope with 4 laser lines (405/488/555/639 nm) with either a 20×/0.8 N.A. air or 63×/1.15 N.A. oil immersion objectives. Images were captured using an AxioCam MRm monochromatic CCD camera (Zeiss) run by Zeiss Zen software.

3. Results

With the aim to determine whether mice expressing ALS-linked mutations in TDP-43 (*prnp*-TDP-43^{Q331K}, hereafter referred as Q331K mice) can be used as a model for ALS-FTD and AD spectrum diseases, we systematically characterized the motor and cognitive phenotypes in a longitudinal manner, that is, the same mouse was tested at 3, 6, and 12 months of age. To discern any potential gender effect, both males and females from the transgene animals and their littermate controls were used and analyzed in this study. A total of 9 Q331K females, 6 Q331K males, 6 nontransgenic females, and 7 nontransgenic males were used. For motor functions, rotarod, balance beam, and open field tests were utilized, whereas for cognitive functions, novel objection recognition, social transmission of food preference, spontaneous alternation in the Y-maze, spatial working memory test using the water maze, hidden platform in the Morris water maze, and contextual fear conditioning were used (Fig. 1; also see the following sections).

3.1. Mice expressing ALS-linked mutation in TDP-43 develop early and persistent motor phenotypes

For characterizing motor phenotypes of Q331K mice, we used rotarod and balance beam tests for assessing motor learning and coordination and the open field test for locomotor activity at 3, 6, and 12 months of age (Figs. 1–3).

3.1.1. Assessment of motor coordination and learning using the rotarod

Animals were run on the rotarod for 5 days and their latencies to fall were recorded (Fig. 2; Supplementary Fig. 1). The GLMER analysis of the latencies to fall showed significant main effects of genotype, age, and test day, with no significant main effect of gender. There were significant interactions between genotype by age, gender by age, age by test day, and genotype by gender by age (Table 1).

For nontransgenic mice, the learning curve at 3 months was significantly steeper than those at 6 months ($p = 0.0052$), and close to significantly steeper than at 12 months ($p = 0.0933$, Fig. 2). Comparing between male and female nontransgenic mice, there were no significant differences in learning curves between the genders at all 3 ages (Supplementary Fig. 1). For Q331K mice, there were no significant differences in the learning curve at all 3 ages (Fig. 2). Comparing between male and female Q331K mice, there were no significant differences in the learning curves at all 3 ages (Supplementary Fig. 1). Pairwise comparisons of means between genotype showed that Q331K mice performed significantly poorer than nontransgenic mice at all 3 ages across test days ($p < 0.0001$; Fig. 2A–C).

The results of the rotarod suggested that Q331K mice developed a motor coordination deficit from as early as 3 months of age and persisted through to 12 months of age.

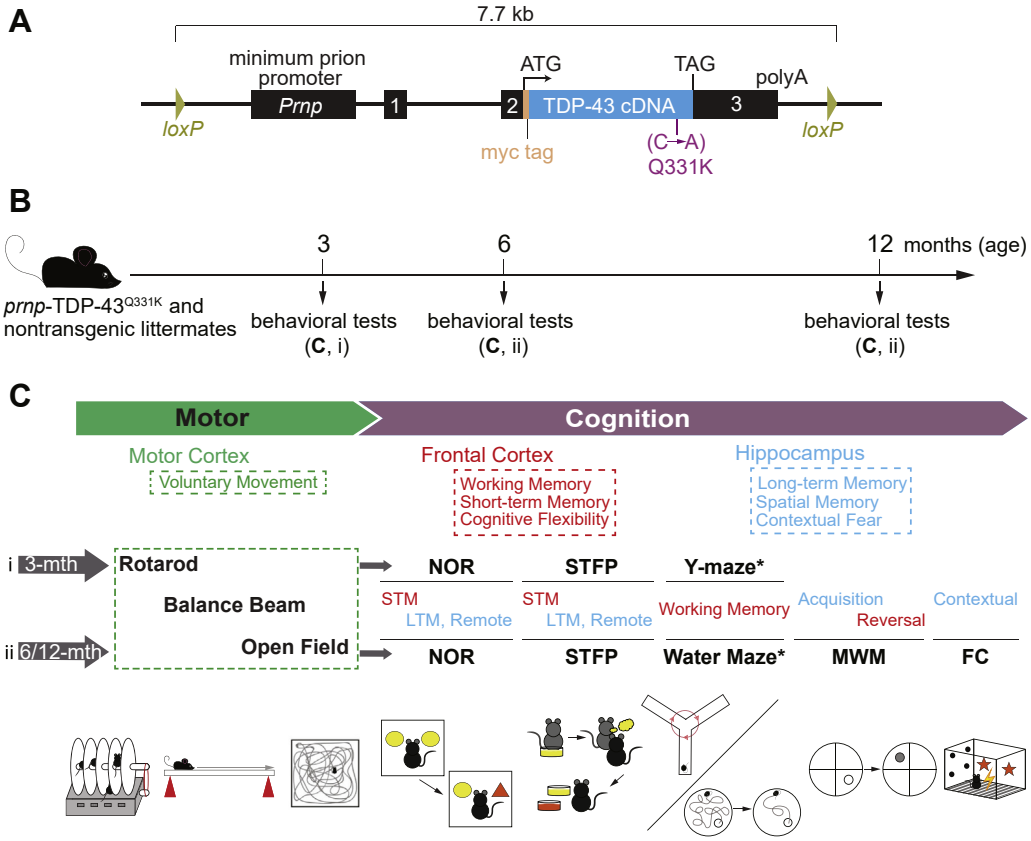

Fig. 1. Summary of the behavioral tests that were performed on *prnp*-TDP-43^{Q331K} and nontransgenic littermates, and the sequence in which they were performed at 3, 6, and 12 months of age. (A) Schematic of TDP-43 transgene. Murine prion promoter was used to drive the myc-tagged human TDP-43 cDNA expression. (B) A schematic summary of the sequence in which the motor and cognitive tests were carried out with schematics of the methodology of the various cognitive tests. *At 3 months, the spatial working memory of mice was assessed using the spontaneous alternation in the Y-maze, and at 6 and 12 months, it was assessed using the water maze. (C) The list of tests that the animals were subjected to, being grouped into the associated brain regions. Motor cortex–associated tests (in green) included the rotarod, balance beam, and open field. Frontal cortex–associated tests (in red) included the short-term memory probes for the novel object recognition and social transmission of food preference tests, the spontaneous alternation in the Y-maze (assessed at 3 months of age), working memory in the water maze (assessed at 6 and 12 months of age), and the reversal paradigm of the Morris water maze task. Hippocampus-associated tasks (in light blue) included the long-term and remote probes, where consolidation and recall processes are involved, of the novel object recognition and social transmission of food preference tests, the fixed platform acquisition task of the Morris water maze, and contextual fear conditioning. Abbreviations: NOR, novel object recognition; STFP, social transmission of food preference; Y-maze, Y-maze spontaneous alternation; WM, water maze; MWM, Morris water maze; FC, fear conditioning; STM, short-term memory; LTM, long-term memory; remote, remote memory. (For interpretation of the references to color in this figure legend, the reader is referred to the Web version of this article.)

3.1.2. Assessment of motor coordination and balance using the 6 mm and 12 mm balance beam

The animals were trained and tested on their abilities to cross 6 mm and 12 mm beams across 5 days. Their latencies to reach safety (the escape box) were recorded (Fig. 2D–I; Supplementary Fig. 2). The GLMER analysis of the latencies to cross the 6 mm and 12 mm beams showed significant main effects of genotype, age, and test day, with no significant main effect of gender (Table 2). For the 12 mm beam, there were significant interactions between genotype by gender, genotype by age, genotype by test day, age by test day, genotype by gender by age, and genotype by gender by test day, whereas for the 6 mm beam, there were significant interactions between genotype and age, genotype and test day, gender by age, and age by test day (Table 2).

Comparing within nontransgenic mice across ages, there was no difference in their performance across the 3 ages on both the 12 mm and 6 mm beams (Fig. 2D–I). Within each age group, there were no significant differences in performances between male and female nontransgenic mice on the 12 mm and 6 mm beams (Supplementary Fig. 2). Within Q331K mice, the learning curves at 6 and 12 months are significantly different compared with at 3 months on the 12 mm beam (ps<0.01, Fig. 2D–F), whereas the performance at 6 months was significantly different from that at 3 and 12 months on the 6 mm beam (Fig. 2G–I). There were no significant differences between male and female Q331K mice at each age group on both 6 mm and 12 mm beams (Supplementary Fig. 2A–L).

Comparing between genotypes, on the 12 mm beam, compared with nontransgenic mice, Q331K mice had significantly longer latencies across test days at all 3 age groups (ps $<$ 0.005, Fig. 2D–F). On the 6 mm beam, compared with nontransgenic mice, Q331K mice had significantly poorer performances at 3 and 6 months of age (ps $<$ 0.005), but not at 12 months old (Fig. 2G–I). Within female mice, Q331K mice performed significantly poorer than nontransgenic mice at all 3 age groups (ps $<$ 0.001; Supplementary Fig. 2A–C) on the 12 mm beam. While on the 6 mm beam, Q331K mice performed significantly poorer than nontransgenic mice at 3 and 6 months (ps $<$ 0.005), but no difference is observed at 12 months (Supplementary Fig. 2H–I). Within male mice, Q331K mice performed significantly poorer at 3 months ($p = 0.0003$), with no different at 6 and 12 months, compared with nontransgenic mice on the 12 mm beam (Supplementary Fig. 2D–F). While on the 6 mm beam, Q331K mice performed significantly poorer than nontransgenic mice at 3 months ($p = 0.0011$), but no different is

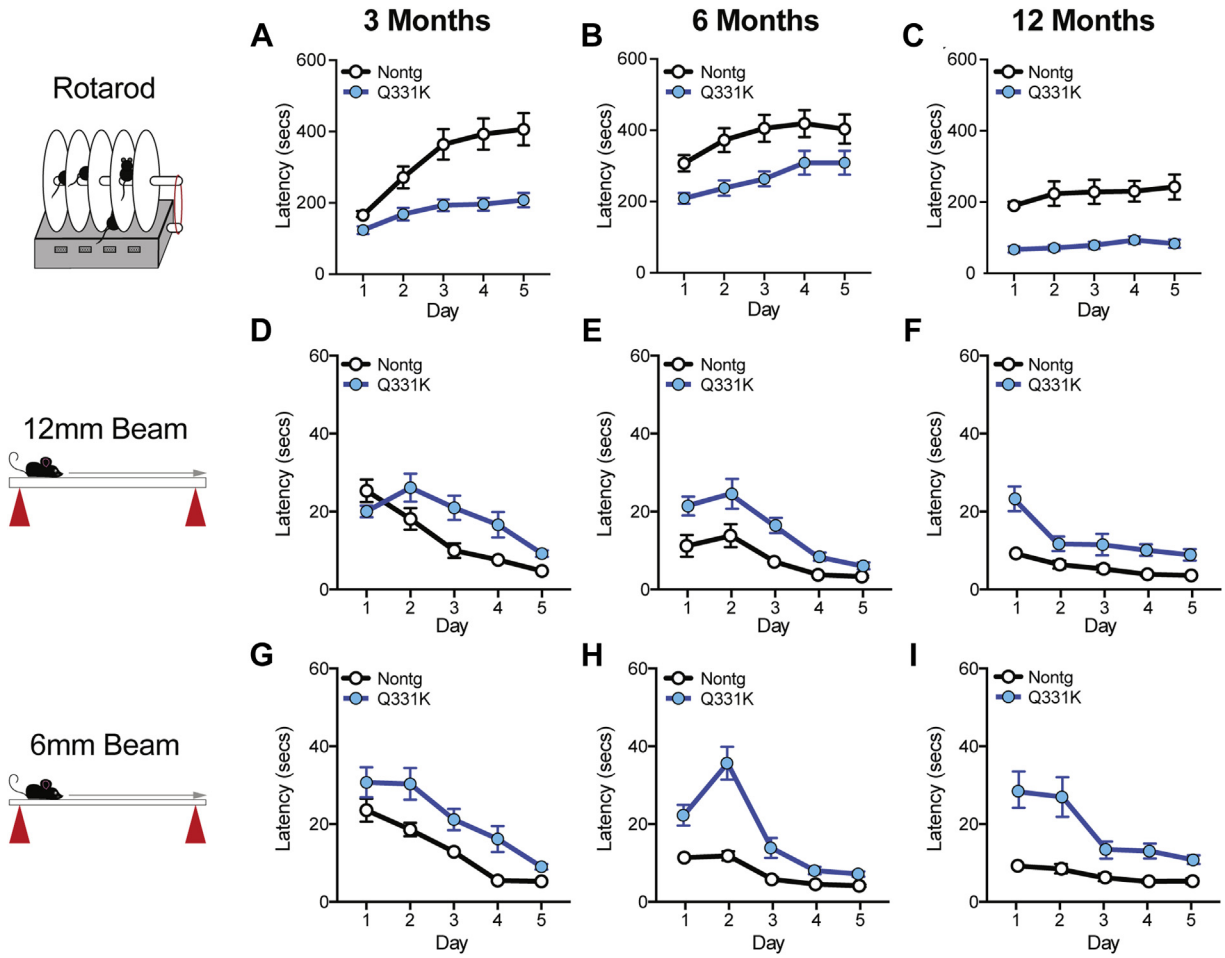

Fig. 2. Early and persistent motor phenotypes in Q331K mice. Q331K mice show deficits in motor coordination and learning at 3, 6, and 12 months of age. (A–C) Latencies to fall in the rotarod test for Q331K and nontransgenic mice. Starting from 3 months of age, Q331K mice showed shorter latencies to fall across the test days than nontransgenic mice ($p < 0.0001$). These poor performances of Q331K mice persisted through to 6 and 12 month-old, with the latencies for Q331K mice to fall on the last test day being significantly lower than nontransgenic mice (ps < 0.05). (D–F) Latencies taken to cross the 12 mm balance beam from Q331K and nontransgenic mice. At 3 and 6 months of age, Q331K mice took longer to across the 12 mm beams across test days than nontransgenic mice ($p = 0.0243$ and $p = 0.0513$, respectively). (G–I) Latencies taken to cross the 6 mm balance beam for Q331K and nontransgenic mice. At 3 mo of age, there were no significant differences in performances between Q331K and nontransgenic mice on the 6 mm beam. Deficits in motor coordination of the Q331K mice on the 6 mm beam showed at 6 and 12 months of age, with poorer performances compared to non-transgenic mice (ps < 0.008). For these tests, there were 15 Q331K mice and 13 nontransgenic mice. Blue circles represent Q331K mice and white circles represent nontransgenic mice. (For interpretation of the references to color in this figure legend, the reader is referred to the Web version of this article.)

observed at 6 and 12 months (Supplementary Fig. 2J–L). Taken together, the results from the balance beams suggested that Q331K mice showed deficits in fine motor coordination from as early as 3 months of age and persisted through to 12 months of age.

As the weights of the mice may affect their performances on the rotarod and balance beams, the weights of mice were recorded at each time point when they underwent testing. At 3 months of age, there was no significant difference in weights between the genotypes, with nontransgenic mice weighing 21.2 (±2.8) grams and Q331K mice weighing 22.8 (±4.2) grams. At 6 months of age, the difference in weights between genotypes was close to significance ($p = 0.0800$), with nontransgenic mice weighing 27.4 (±4.2) grams and Q331K mice weighing 30.2 (±3.6) grams. At 12 months of age, there was a significant difference in weights between genotypes ($p = 0.00784$), with nontransgenic mice weighing 35.8 (±6.9) grams and Q331K mice weighing 42.8 (±5.5) grams. The observed motor deficits in the rotarod and balance beams were not due to the weight differences between nontransgenic and Q331K mice because the motor deficits were early onset and persistent, whereas the weight differences only occurred after 6 months of age.

3.1.3. Assessment of exploratory and locomotor activity in the open field

Animals were placed in a square open field box for 60 minutes and their distances traveled were recorded by the Topscan analysis program (Fig. 3; Supplementary Fig. 3). The data for distance traveled in the open field are presented as distance traveled per 5 minutes time bin (Fig. 3A–C, Supplementary Fig. 3A–F) or cumulative distance traveled over 60 minutes (Fig. 3D–F, Supplementary Fig. 3G–L). The LMER analysis of distance traveled per 5 minutes showed significant main effects of genotype, time, and interactions of genotype by age, genotype by gender, genotype by time, age by time, genotype by gender by age, and genotype by age by time. The LMER analysis of cumulative distance traveled over 60 minutes showed significant main effects of genotype and age and significant genotype by gender interaction (Table 3).

Pairwise comparisons with the cumulative distances traveled over 60 minutes showed that Q331K mice traveled a significantly reduced distance compared with the nontransgenic counterparts at all 3 ages (ps < 0.02, Fig. 3D–F). Within genotypes, there were no significant differences between male and female nontransgenic

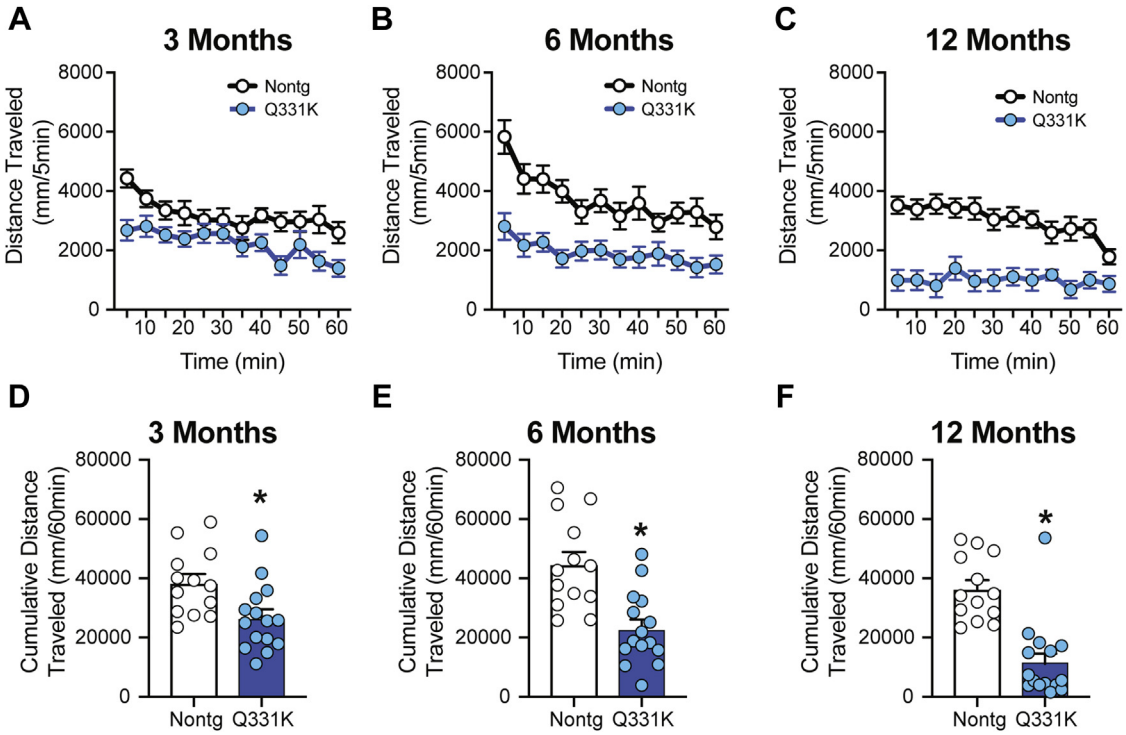

Fig. 3. Reduced locomotor activities in Q331K mice. Q331K mice show reduced locomotor activity in the open field at 3, 6, and 12 months show reduced locomotor activity in Q331K mice. (A–C) Distances traveled in the open field per 5-min blocks. (D–F) Cumulative distance traveled in the open field for 60 min. At all 3 ages, Q331K mice had reduced distances traveled compared with nontransgenic mice (ps < 0.02). For these tests, there were 15 Q331K mice and 13 nontransgenic mice. Blue circles and bars represent Q331K mice, and white circles and bar represent nontransgenic mice. *$p < 0.05$ between genotypes. (For interpretation of the references to color in this figure legend, the reader is referred to the Web version of this article.)

mice at all 3 ages (Supplementary Fig. 3G–L). For females, Q331K mice had significantly reduced distances traveled compared with nontransgenic mice at 6 and 12 months of age (ps < 0.001), but not at 3 months of age (Supplementary Fig. 3G–I). For males, there were no significant differences in distances traveled between nontransgenic and Q331K mice at all 3 ages (Supplementary Fig. 3J–L). The results from the open field suggested that female, but not male, Q331K mice showed age-dependent reduction in locomotor activity.

3.2. Mice expressing ALS-linked mutation in TDP-43 are comparable with their nontransgenic littermates in hippocampus-dependent cognitive tests

To determine whether these Q331K mice developed hippocampus-mediated cognitive deficits, we performed the hidden platform water maze paradigm to assess spatial memory and contextual fear conditioning to assess contextual fear memory at 6 and 12 months of age (Supplementary Figs. 4 and 5).

Table 1
Generalized linear mixed effect model results for latencies to fall in the rotarod

Latency to fall	Effect	Chi Sq	Df	*p*
Rotarod	Genotype	44.6	1	<0.0001
	Age	249	2	<0.0001
	Test day	40.6	1	<0.0001
	Geno × age	124	2	<0.0001
	Gender × age	22.1	2	<0.0001
	Age × test day	10.1	2	0.00653
	Genotype × gender × age	47.4	2	<0.0001

Degrees of freedom were calculated using the type II Wald chi-square test.

3.2.1. Assessment of spatial acquisition and memory in the hidden platform Morris water maze paradigm

The animals were trained in a hidden platform paradigm of the Morris water maze where they could only rely on distally placed spatial cues to find the escape platform (Fig. 4A). They were trained for 4 trials a day for 5 days. There were 2 probes. The first occurred 20 minutes after the first training for STM, and the second occurred 16–24 hours after the last training for LTM (Fig. 4B–C; Supplementary Fig. 4). We observed that Q331K female mice had

Table 2
Generalized linear mixed effect model results for latencies to reach the escape box for 12 mm and 6 mm beams

Latency to reach the escape box	Effect	Chi Sq	Df	*p*
12 mm beam	Genotype	16.2	1	<0.0001
	Age	81.7	2	<0.0001
	Test day	225	1	<0.0001
	Genotype × gender	7.00	1	0.00815
	Genotype × age	13.8	2	0.00102
	Genotype × test day	42.3	1	<0.0001
	Age × test day	22.8	2	<0.0001
	Genotype × gender × age	42.3	2	<0.0001
	Genotype × gender × test day	7.30	1	0.00689
6mm beam	Genotype	54.5	1	<0.0001
	Age	27.3	2	<0.0001
	Test day	239	1	<0.0001
	Genotype × gender	7.33	1	0.00676
	Genotype × age	31.7	2	<0.0001
	Genotype × test day	25.4	1	<0.0001
	Gender × age	13.7	2	0.00105
	Age × test day	8.96	2	0.0113
	Genotype × gender × age	16.2	2	0.000304

Degrees of freedom were calculated using the type II Wald chi-square test.

Table 3
Separate linear mixed effect model results for distances traveled per 5 min or cumulative distance traveled over 60 min

Distance traveled	Effect	Dfs	F(Df)	*p*
Per 5 min time bin	Genotype	1, 111	66.4	<0.0001
	Age	2, 112	9.60	0.000142
	Time	1, 918	182	<0.0001
	Genotype × age	2, 112	5.44	0.00558
	Genotype × gender	1, 113	17.3	<0.0001
	Genotype × time	1, 912	20.3	<0.0001
	Age × time	2, 912	6.29	0.00192
	Genotype × age × time	2, 912	5.80	0.00314
	Genotype × gender × age	2, 113	3.49	0.0340
Per 60 min	Genotype	1, 72	56.2	<0.0001
	Age	2, 72	5.26	0.000142
	Genotype × gender	1, 72	16.4	0.00123

Degrees of freedom were calculated using Satterthwaite's method.

poor latencies to reach the platform during the water maze spatial acquisition and reversal tasks at 12 months of age because they spent most of the trial floating in the water. We also noted that if their data were included in the data analysis, the homogeneity of variance was violated. Hence, the data from all 12-month-old female mice were excluded from the analysis. At the end testing session, we observed that Q331K female mice were able to swim to the tester's hand to be taken out of the water maze, suggesting that their swimming abilities were not impeded, but rather, they lacked the motivation to carry out the task.

The LMER analysis of the time spent in target quadrant during the probe trials showed significant main effects of probe day (Table 4). There were no significant pairwise comparisons within or between genotype and age (Fig. 4B–C). The average distance traveled during the probe trials were analyzed as a measure of the levels of exploratory activity exhibited by mice during the water maze spatial acquisition test (Table 5). The analysis of distance traveled during the probe trials showed a significant main effect of age (Table 5), with a close to significant genotype by age interaction ($p = 0.0617$). Pairwise comparisons of distance traveled during probe trials showed that within each genotype, mice swam for significantly longer distances at 12 months compared with at 6 months of age (ps < 0.04). In addition, nontransgenic mice swam for significantly longer distances than Q331K mice during the probe trials at 12 months ($p = 0.0476$).

3.2.2. Assessment of contextual fear memory

The animals were placed in an operant chamber where they received an aversive stimulus through a scrambled foot-shock during training (Fig. 4D). They were then assessed for their retention of contextual fear memory through 3 probes (STM, LTM, and RM), which were carried out 20 minutes, 16–24 hours, and 10–14 days, respectively, after training. The time spent freezing in the operant chamber was recorded (Fig. 4E–F; Supplementary Fig. 5).

The LMER analysis of the percentage time spent freezing during the probes showed an almost significant main effect of genotype (Table 6; Fig. 4E–F). There were no significant comparisons found at 6 or 12 months of age between or within genotype.

The results from the spatial acquisition task in the Morris water maze suggested that spatial memory of Q331K mice was intact and the results from the contextual fear conditioning suggested that contextually derived fear memory of Q331K mice was intact. Taken together, the hippocampus-dependent memory function of Q331K mice was not impaired, as assessed by these 2 tests.

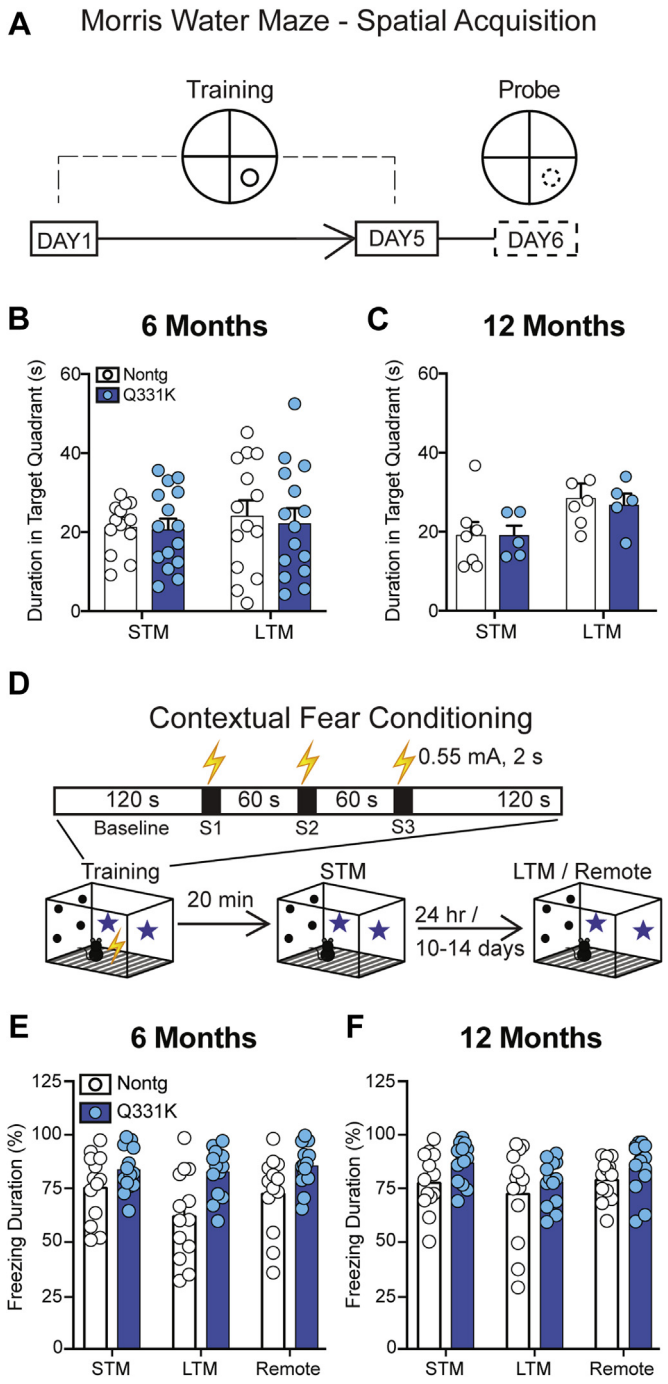

Fig. 4. Morris water maze and contextual fear conditioning test probes. Q331K mice show no deficits in hippocampus-dependent cognitive tasks at 6 and 12 mo. (A) A schematic showing he Morris water maze spatial acquisition paradigm that was used to assess the hippocampus-dependent acquisition of spatial memory. (B–C) Two probe tests were performed, with the short-term memory probe carried out 20 min after the first training session and the long-term memory probe carried out 16–24 h after the fifth training session. There were no significant differences in the amount of time spent in the target quadrant between Q331K and nontransgenic mice. (D) A schematic showing the contextual fear conditioning paradigm that was used to assess hippocampus-dependent contextually acquired fear memory. (E–F) Percentages of freezing during probes were recorded during the contextual fear conditioning paradigm. There were no significant differences in the percentages of time spent freezing between Q331K and nontransgenic mice across all 3 ages. For all the tests shown here, except for the Morris water maze at 12 mo, there were 15 Q331K mice and 13 nontransgenic mice. Blue circles and bars represent Q331K mice, and white circles and bar represent nontransgenic mice. For the Morris water maze tests at 12 mo, the data presented here are from male mice only. (For interpretation of the references to color in this figure legend, the reader is referred to the Web version of this article.)

Table 4
Separate linear mixed effect model results for latencies to reach platform during training days and distances traveled in acquisition and probe trials in the water maze spatial acquisition test

Water maze spatial acquisition	Effect	Dfs	F(Df)	*p*
Latency to reach the platform during training	Training day	1, 196	6.34	0.0219
	Genotype × training day	1, 196	11.6	0.000807
Time spent in the target quadrant during probes	Probe day	1, 37	5.11	0.0298
Distance traveled during training	Genotype	1, 19.5	5.15	0.0349
Distance traveled during probes	Age	1, 24.7	30.4	<0.0001

Degrees of freedom were calculated using Satterthwaite's method.

Table 6
Separate linear mixed effect model results for percentages of time spent freezing during the contextual fear conditioning training and probe days

Percentage of time spent freezing	Effect	Dfs	F(Df)	*p*
Learning curve	Genotype	1, 183	14.2	0.000222
	Shock progression	1, 157	144	<0.0001
	Genotype × gender	1, 183	4.98	0.0268
	Genotype × shock progression	1, 157	14.5	0.000196
	Age × shock progression	1, 157	3.28	0.0720
Probe days	Genotype	1, 155	3.53	0.0620

Degrees of freedom were calculated using Satterthwaite's method.

3.3. Mice expressing ALS-linked mutation in TDP-43 developed early and persistent cognitive deficits that are associated with the frontal cortex

TDP-43 pathology is associated with FTD patients, who are characterized by the degeneration of their frontal and temporal lobes. Correspondingly, the executive functions and higher cognition functions were impaired in patients with FTD (Nag et al., 2015). Thus, we characterized the frontal cortical functions of Q331K mice and their nontransgenic counterparts by performing a battery of cognitive tests that assessed short-term recognition and socially acquired memory, spatial working memory, and cognitive flexibility at 3, 6, and 12 months of age (Fig. 1).

3.3.1. Assessment of recognition memory in the novel object recognition test

The animals were first trained with 2 identical objects. Subsequently, the animals were probed at 20 minutes, 16–24 hours, and 10–14 days later for STM, LTM, and RM, respectively, whereby one familiar object was switched out for a novel object (Fig. 5A). The duration spent interacting with each object was recorded and the preference scores for the novel object were calculated (Fig. 5B–D; Supplementary Fig. 6).

The GLMER analysis for the percentage time spent with the novel object showed a significant main effect of genotype and test day, with a significant genotype by test day and gender by age and test day interactions (Table 7). Pairwise comparisons within each genotype showed that, at all ages, nontransgenic mice showed significantly higher preference scores for the novel object at STM, LTM, and RM compared with training (ps < 0.05; Fig. 4B–D). At all 3 ages, Q331K mice showed significantly higher preference for the novel object at LTM and RM (ps < 0.05), but the preference scores at STM were not significantly different from training (Fig. 5B–D).

Pairwise comparisons between genotypes showed that, on the training day, there were no significant differences in preferences between both nontransgenic and Q331K mice at all 3 ages. For STM, Q331K mice showed significantly lowered preferences for the novel object than nontransgenic mice at all 3 ages (ps < 0.005). For LTM and RM, both nontransgenic and Q331K mice showed similar levels of preference for novel object at all 3 ages. To ensure that the significantly reduced preference for the novel object shown by Q331K mice compared with nontransgenic at STM across was not due to different exploration levels between genotypes, the total time spent across both objects were analyzed. The total time spent interacting with the objects per session was 46.3 (±3.00) seconds for nontransgenic mice and 45.5 (±6.13) seconds for Q331K mice. For the total time spent interacting with the objects, there was no significant main effects of genotype, gender, age, or test day. The data suggested that Q331K mice showed an impaired short-term recognition memory, which is associated with the frontal cortex, from as early as 3 months of age and persisted through to 12 months of age, whereas LTM and RM, which are associated with the hippocampus, were mostly intact.

3.3.2. Assessment of socially acquired memory in the social transmission of food preference test

The animals were introduced to a familiar scented diet and then probed for memory of the familiar scent 20 minutes, 16–24 hours, and 10–14 days later for STM, LTM, and RM memory, respectively (Fig. 5E). The amount of each food consumed was recorded and the amount of familiar food consumed as a percentage of total food consumption was calculated (Fig. 5F–H; Supplementary Fig. 7). It was noted that 12-month-old Q331K female mice refused to consume any food from either diet for RM, even though they were observed to start eating on their return to the home-cage after the probe, suggesting that they were hungry. These mice also had no previously observed issues with consuming test food during the earlier testing time points, at 3 and 6 months of age. As the 12-month-old Q331K female mice had such poor performance in the task, their data were not sufficiently robust for us to address our hypothesis and the inclusion of their data resulted in

Table 5
Means and standard deviations for distances traveled during the spatial acquisition training and probe trials for the water maze

Trial type	Genotype	Gender	Age (mo)	Average (mm)	± SEM
Training	Nontg	Female	6	366	102
			12	N.A.	N.A.
		Male	6	248	67.8
			12	293	35.2
		Combined	6	303	60.0
			12	293	35.2
	Q331K	Female	6	502	46.7
			12	N.A.	N.A.
		Male	6	281	60.3
			12	404	34.9
		Combined	6	454	39.0
			12	404	34.9
Probe	Nontg	Female	6	508	41.6
			12	N.A.	N.A.
		Male	6	373	38.0
			12	907	93.2
		Combined	6	436	33.2
			12	907	93.2
	Q331K	Female	6	389	31.4
			12	N.A.	N.A.
		Male	6	521	143
			12	684	77.9
		Combined	6	442	59.6
			12	684	77.9

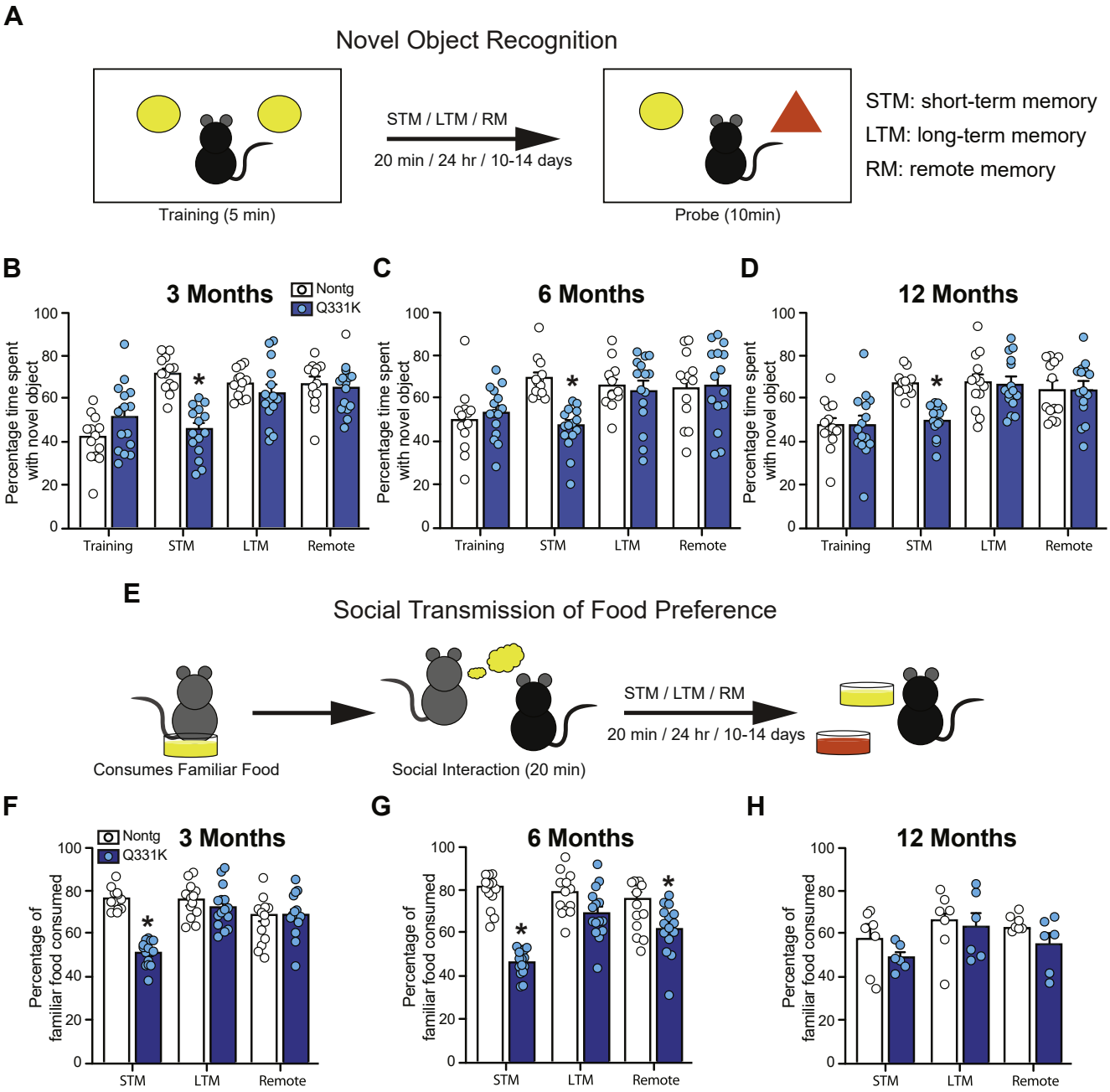

Fig. 5. Q331K mice show short-term memory deficits. (A) A schematic showing the novel object recognition paradigm. (B–D) Q331K mice showed significantly lower time spent with the novel object than nontransgenic mice for STM at all 3 ages (ps < 0.002). This reduced time spent with the novel object shown by Q331K mice was not due to different exploration levels between genotypes as the total time spent interacting with both objects were similar between genotypes. (E) A schematic showing the social transmission of food preference paradigm. (F–H) Q331K mice showed reduced percentage consumption of the familiar diet at 3 and 6 months of age (ps < 0.0001). Although Q331K mice showed a reduced percentage consumption of the familiar diet at 12 months of age, this was not significantly different from nontransgenic mice ($p = 0.120$). For all the tests shown here, except for the social transmission of food preference tests at 12 mo, there were 15 Q331K mice and 13 nontransgenic mice. Blue circles and bars represent Q331K mice, and white circles and bar represent nontransgenic mice. For the social transmission of food preference tests at 12 months of age, the data presented here are from male mice only (6 Q331K, 7 nontransgenic). *$p < 0.05$ between genotypes. (For interpretation of the references to color in this figure legend, the reader is referred to the Web version of this article.)

heteroscedasticity. Hence, the data from 12-month-old female mice were excluded in the analysis.

The LMER analysis of the amount of familiar diet consumed as a percentage of total food consumed showed significant main effects of genotype, age, and test day, and significant genotype by age, genotype by test day, and genotype by age by test day interaction (Table 8). Pairwise comparisons showed that at all 3 ages, nontransgenic mice showed similar percentage consumption of the familiar diet across the STM, LTM, and RM probes (Fig. 5F–H). At 3 and 6 months, Q331K mice showed significantly reduced percentage consumption of the familiar diet at STM compared with LTM and RM at each age (ps $<$ 0.0001; Fig. 5F–H). At 12 months, Q331K mice showed significantly reduce percentage consumption of the familiar diet at STM compared to LTM ($p = 0.0276$), but not at RM (Fig. 5H).

Comparing between genotypes, pairwise comparisons for STM showed that Q331K had significantly lowered percentage consumption of the familiar diet compared with nontransgenic mice at 3 and 6 months of age (ps < 0.0001; Fig. 5F–G), but not at 12 months of

Table 7
Generalized linear mixed effect model results for percent time spent with novel object in the novel object recognition test

Novel object recognition	Effect	Chi Sq	Df	*p*
Percentage time spent with novel object	Genotype	8.37	1	0.00382
	Test day	95.8	3	<0.0001
	Genotype by test day	62.0	3	<0.0001
	Age × gender × test day	12.6	6	0.0496

Degrees of freedom were calculated using the type II Wald chi-square test.

age ($p = 0.120$; Fig. 5H). In addition, at 6 months of age, Q331K mice had significantly lower percentage consumption of the familiar diet compared with nontransgenic mice during RM ($p = 0.0029$). To ensure that the differences observed previously were not due to differences in food consumption between genotypes, the amount of food consumed were analyzed. The average total amount of food consumed for each test session was 0.697 (±0.0360) grams for nontransgenic mice and 0.596 (±0.0338) grams for Q331K mice. There were no significant main effects or interactions. There were otherwise no significant differences in preferences for the familiar diet between nontransgenic and Q331K mice at LTM and RM at 3 and 12 months of age. Pairwise comparisons between male and female mice of each genotype showed no significant differences in preferences across all test days and ages. Taken together, the data suggested that Q331K mice showed impaired STMs in socially acquired memory, which is associated with the frontal cortex. Social transmission of food preference assay from as early as 3 months of age and the deficits persist through to 12 months of age, whereas LTM and RM, which are associated with the hippocampus, were mostly intact.

3.3.3. *Assessment of spatial working memory*

To characterize the frontal cortical function of Q331K mice, the spatial working memories of Q331K and nontransgenic mice were measured using 2 behavioral paradigms (Fig. 1). At 3 months old, spontaneous alternation in the Y-maze test was used. To further confirm the deficits in working memory, spatial working memory in the water maze paradigm was used at 6 and 12 months of age (Fig. 6A and C).

In the spontaneous alternation of the Y-maze, animals were allowed to freely explore a Y-shaped maze for 10 minutes and the arm entries were recorded to obtain the percentage of alternations (Fig. 6A, Supplementary Fig. 8A–B). The LMER analysis of percentage of alternations in the Y-maze showed significant main effects of genotype only for 3-month-old mice (p=0.00783). There was no significant main effect of gender (Fig. 6B, Table 9). Within genotype, there were no differences between female and male nontransgenic mice. For Q331K mice, female mice had significantly higher percentage of alternations than male mice ($p = 0.0375$, Supplementary Fig. 8A–B). Between genotypes, female Q331K mice showed an almost significant lowered percentage of alternations compared with female nontransgenic mice ($p = 0.0751$). Male Q331K mice had a significantly lowered percentage of alternations compared with male nontransgenic mice ($p = 0.0017$). To ensure that the deficiency in Q331K mice at 3 months was not due to a lack of exploration in the maze, the total number of arm entries was calculated. The average

Table 8
Separate linear mixed effect model results for preference scores in the social transmission of food preference test

Social transmission of food preference	Effect	Dfs	F(Df)	*p*
Preference scores	Genotype	1, 59	32.5	<0.0001
	Age	2, 59	5.63	0.00579
	Test day	2, 118	14.2	<0.0001
	Genotype × test day	2, 118	11.7	<0.0001

Degrees of freedom were calculated using Satterthwaite's method.

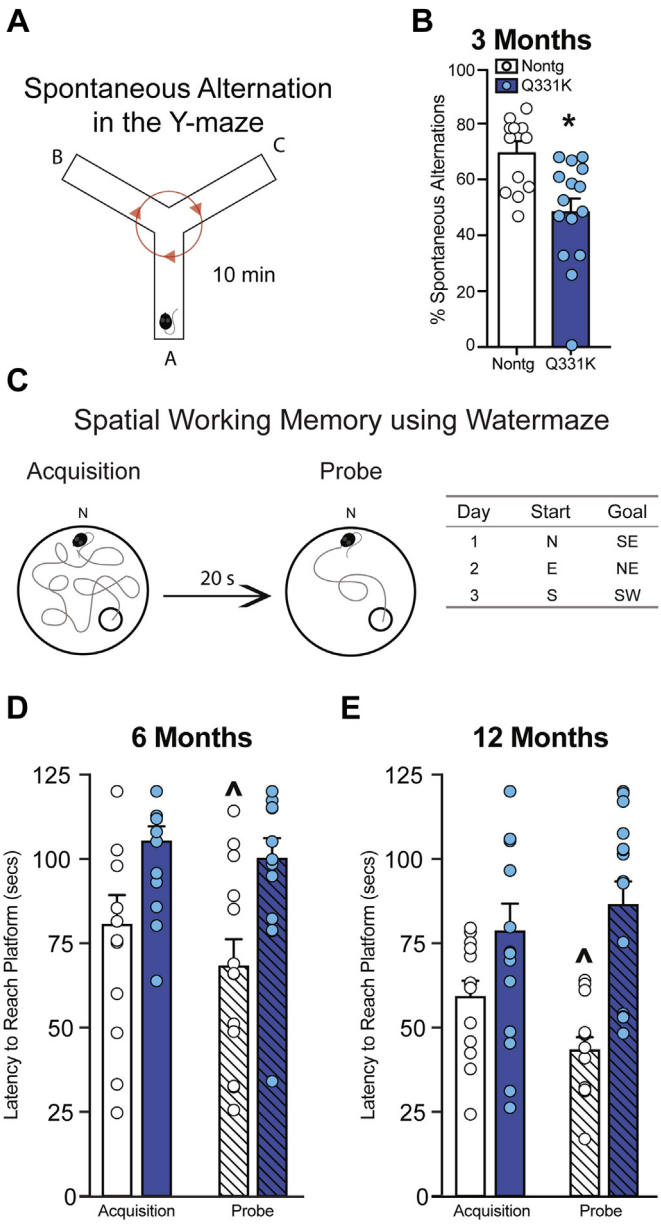

Fig. 6. Q331K mice show deficits in spatial working memory. (A) A schematic showing the spontaneous alternation in the Y-maze paradigm. (B) Q331K mice showed a reduced percentage of spontaneous alternations in the Y-maze compared with nontransgenic mice at 3 months of age ($p = 0.00783$). (C) A schematic showing the spatial working memory in the water maze paradigm. (D–E) The latencies to reach the platform during the acquisition and probe trials were recorded. Q331K mice did not show any significant reductions in the latencies to reach platform during probe trials. However, nontransgenic mice showed significant reductions in the latencies to reach platform ($p < 0.05$). For all tests shown here, there were 15 Q331K mice and 13 nontransgenic. Blue circles and bars represent Q331K mice, and white circles and bar represent nontransgenic mice. *$p < 0.05$ between genotypes; ^$p < 0.05$ between acquisition and probe trials. (For interpretation of the references to color in this figure legend, the reader is referred to the Web version of this article.)

number of arm entries for nontransgenic mice was 26.1 (±1.33) and for Q331K mice was 23.3 (±1.57). The total number of arm entries showed no significant main effects or interactions.

At 6 and 12 months of age, Q331K mice and their nontransgenic counterparts underwent spatial working memory in the water maze paradigm. In this hidden platform test, there were 4 trials that were separated by a 20-second intertrial interval. The first trial was taken to be the acquisition trial and the subsequent 3 trials were taken to be probe trials. The release and platform locations of the

Table 9
Separate linear mixed effect model results for the percentage of alternations and the number of arm entries in the Y-maze

Y-maze	Effect	Dfs	F(Df)	*p*
Percentage of alternations	Genotype	1, 24	14.8	0.000783

Degrees of freedom were calculated using Satterthwaite's method.

probe trials were kept the same as in the acquisition trial for each day (Fig. 6C). The mice were tested across 3 days.

The LMER analysis of the latencies to reach the platform for all trials showed significant main effects of genotype, age, and trial, with no significant main effect of gender. There were significant interactions of genotype by trial and genotype by age by trial (Table 10). Pairwise comparisons within age for nontransgenic mice showed that the latencies to reach the platform for all probe trials were significantly lower than for their respective acquisition trials (ps < 0.05; Fig. 6D and E). For 6-month-old Q331K mice, there were no significant differences in latencies to reach the platform between the probe and acquisition trials (Fig. 6D). For 12-month-old Q331K mice, the latencies were significantly higher during the second and third probe trials in comparison with the acquisition trial (ps < 0.05; Fig. 6E). Comparing the learning trends of the different ages within genotype showed no significant differences between 6- and 12-month-old nontransgenic mice, whereas Q331K mice at 12 months performed significantly poorer than those at 6 months ($p = 0.0053$). Pairwise comparisons of the acquisition trials across genotypes showed that at 6 months of age, Q331K mice took significantly longer to reach platform than nontransgenic mice ($p = 0.0222$; Fig. 6D, Supplementary Fig. 8C–D). However, the linear trends pairwise comparisons showed that the learning trends between nontransgenic and Q331K mice were not significantly different at 6 months of age ($p = 0.154$). At 12 months of age, the difference in latencies to reach the platform during the acquisition trials between Q331K and nontransgenic mice was almost significant ($p = 0.0853$; Fig. 6E, Supplementary Fig. 8E–F). In addition, the learning curves of Q331K mice were significantly poorer than those of nontransgenic mice ($p < 0.0001$).

To ensure that the latencies to reach the platform was not due to reduced exploration of Q331K mice, the distance traveled during the trials were analyzed. During the acquisition trials, nontransgenic mice traveled 15,373 ± 1471 mm and during the probe trials, they traveled 14,257 ± 1772 mm. Q331K mice traveled 26,940 ± 3888 mm during the acquisition trials and 26,918 ± 4254 mm during the probe trials. For the distance traveled during the acquisition and probe trials in the working memory water maze test, there was only a significant main effect of genotype and a genotype by age interaction (Table 10). There are no significant differences in distance traveled between nontransgenic and Q331K mice at 6 months old. At 12 months old, Q331K mice traveling longer distances than nontransgenic mice during the acquisition and probe trials (ps < 0.02). Hence, exploratory activity was not a confounding factor in the deficits exhibited by the Q331K mice in the working memory water maze task.

Taken together, the data from the Y-maze and the water maze suggested that spatial working memory, which is associated with frontal cortical function, was impaired for Q331K mice from as early as 3 months of age and persisted through to 12 months of age.

3.3.4. Assessment of cognitive flexibility in the spatial reversal hidden platform Morris water maze paradigm

We further characterized the frontal cortical function of Q331K mice by assessing the cognitive flexibility of Q331K mice and their nontransgenic counterparts in the spatial reversal Morris water maze paradigm. After the LTM probe of the spatial acquisition phase was completed, the location of hidden platform in the Morris water maze was changed to the opposite quadrant. Mice were then trained to find the new location for 6 consecutive days (Fig. 7A). There were 2 probes. STM occurred 20 minutes after the first training and LTM occurred 16–24 hours after the last training (Fig. 7F–M; Supplementary Fig. 9).

Table 10
Separate linear mixed effect model results for latencies to reach platform and distances traveled in acquisition and probe trials in the working memory water maze test

Working memory water maze	Effect	Dfs	F(Df)	*p*
Latency to reach the platform	Genotype	1, 51	37.2	<0.0001
	Age	1, 51	7.01	0.0107
	Test day	3, 156	4.54	0.00442
	Genotype × test day	3, 156	8.36	<0.0001
	Genotype × age × test day	3, 156	2.91	0.0362
Distance traveled	Genotype	1, 26.5	6.53	0.0167
	Genotype × age	1, 79.3	8.00	0.00592

Degrees of freedom were calculated using Satterthwaite's method.

The LMER analysis of latencies to reach the platform during the spatial reversal training showed significant main effects of genotype, training day, and significant genotype by training day interaction (Table 11). Pairwise comparisons within genotype showed no gender differences at 6 months of age (Supplementary Fig. 9A–B). Comparisons between genotype showed that at both 6 and 12 months of age, Q331K mice had significantly poorer learning curves compared with nontransgenic mice across training days (ps < 0.002; Fig. 6B and D).

The LMER analysis of time spent in target quadrant during the probe trials showed significant main effects of genotype, probe day, and genotype by probe day. There was no significant main effect of gender and age. Pairwise comparisons showed that male nontransgenic mice spent more time in the target quadrant at LTM compared with STM at both 6 and 12 months of age (ps < 0.05; Supplementary Fig. 9F and H), whereas Q331K mice showed no significant differences in the amount of time spent in the target quadrant between STM and LTM at both ages (Fig. 7C and E). At 6 months of age, Q331K mice spent significantly less time in the target quadrant than nontransgenic mice during LTM ($p = 0.0001$; Fig. 7F), with the difference between genotypes being almost significant during STM ($p = 0.0696$). At 12 months of age, male Q331K mice spent significantly less time in the target quadrant than nontransgenic mice at both STM and LTM (ps < 0.03; Fig. 6E; Supplementary Fig. 9H).

The average distance traveled during training and the probe trials were analyzed as a measure of the levels of exploratory activity exhibited by the mice during the water maze spatial reversal test (Table 12). The analysis of distances traveled during the training trials showed a main effect of genotype and gender, although there were no significant pairwise comparisons. The analysis of distances traveled during the probe trials showed a significant main effect of age, and pairwise comparisons showed that nontransgenic mice swam for significantly longer distances at 12 months than at 6 months old ($p = 0.002$). Taken together, the data revealed that Q331K mice performed worse than nontransgenic mice in the reversal hidden platform assay at both 6 and 12 months of age. This suggests that the frontal cortex–mediated cognitive flexibility capacity may be impaired in Q331K mice.

3.4. Human TDP-43 transgene expresses at the comparable level as the endogenous mouse counterpart without apparent aggregates

As TDP-43 has been shown to autoregulate its own expression by feedback regulation of its own mRNA (Arnold et al., 2013; Polymenidou et al., 2011), we first examined the steady state of mouse TDP-43 mRNA by qRT-PCR. Mouse TDP-43 mRNAs in the

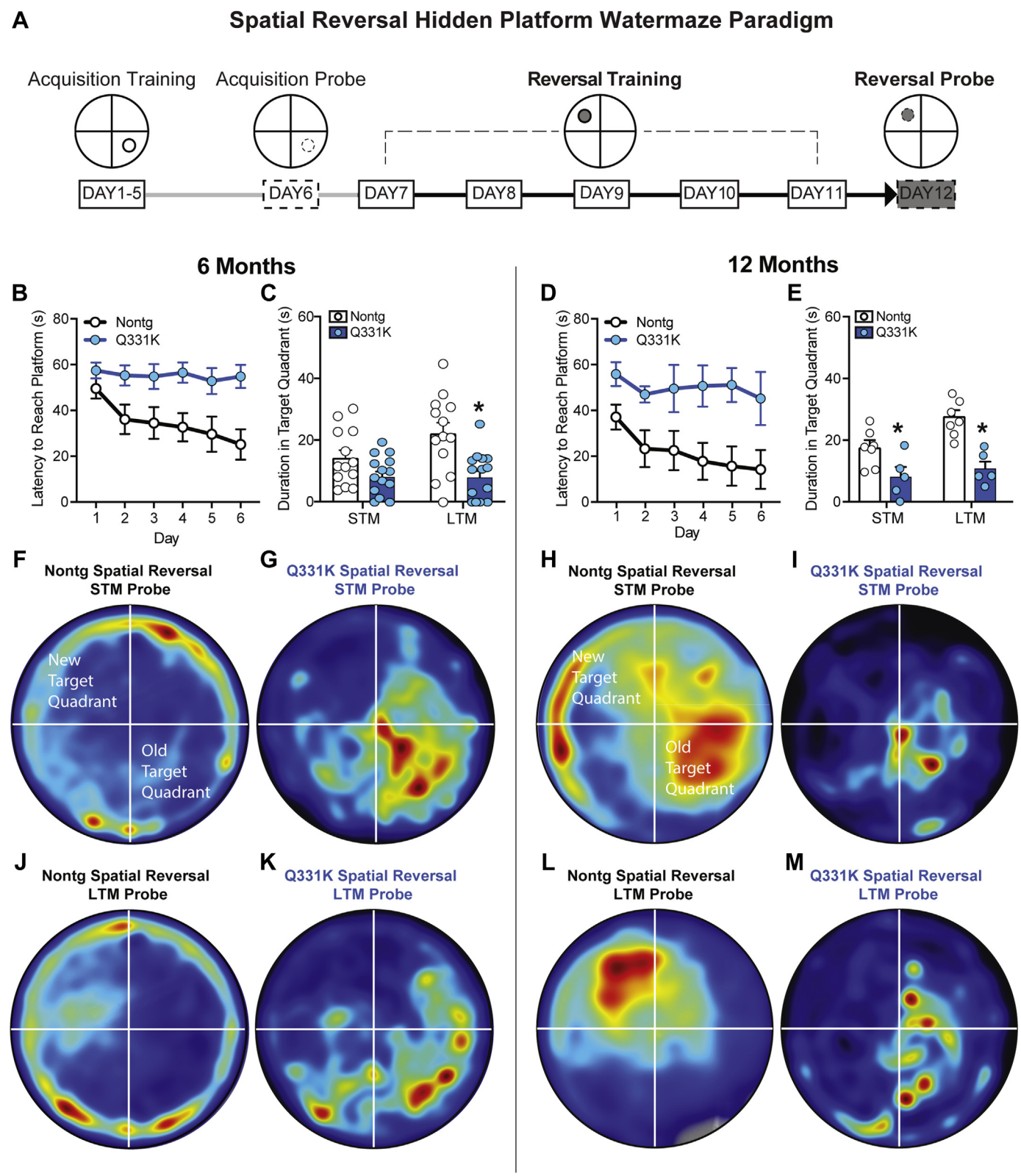

Fig. 7. Q331K mice show deficits in cognitive flexibility. (A) A schematic showing the spatial reversal of the hidden platform in the Morris water maze paradigm. (B–E) The latencies to reach the hidden platform in its new location across the 5 training days are shown in panels B and D. The learning performances of Q331K mice were significantly poorer than nontransgenic mice at both 6 and 12 months of age (ps < 0.002). Two probe tests were performed, as shown in panels C and E, with the short-term memory probe carried out 20 min after the first reversal training session and the long-term memory probe carried out 16–24 h after the 6th reversal training session. During STM, Q331K mice spent less time in the target quadrant than nontransgenic mice at 6- ($p = 0.0696$) and 12- ($p < 0.03$) months of age. During LTM, Q331K mice spent significantly less time in the target quadrant than nontransgenic mice at both 6 and 12 months of age (ps < 0.03). (F–M) The average graphical representation for the search patterns of Q331K and nontransgenic mice during each probe that was carried out at 6 and 12 months. From these graphical representations, it can be seen that Q331K mice tended to persist in the old target quadrant, whereas after 6 days of training, the nontransgenic mice showed increased explorations in the new target quadrant. For the test shown, at 6 months, there were 15 Q331K mice and 13 non-transgenic mice, and at 12 months, the data presented here are from male mice only (5 Q331K, 7 nontransgenic). Blue circles and bars represent Q331K mice, and white circles and bar represent nontransgenic mice. *$p < 0.05$ between genotypes. Abbreviations: STM, short-term memory; LTM, long-term memory. (For interpretation of the references to color in this figure legend, the reader is referred to the Web version of this article.)

Table 11
Separate linear mixed effect model results for latencies to reach the platform during training days and distances traveled in acquisition and probe trials in the water maze spatial reversal test

Water maze spatial reversal	Effect	Dfs	F(Df)	*p*
Latency to reach the platform during training	Genotype	1, 71.5	4.04	0.0483
	Training day	1, 196	22.6	<0.0001
	Genotype by training day	1, 196	9.51	0.00233
Time spent in target quadrant during probes	Genotype	1, 33	23.1	<0.0001
	Probe day	1, 33	8.41	0.00658
	Genotype by probe day	1, 33	5.91	0.0207
Distance traveled during training	Genotype	1, 34	5.30	0.0275
	Sex	1, 34	4.64	0.0385
Distance traveled during probe	Age	1, 34	6.78	0.0136

Degrees of freedom were calculated using Satterthwaite's method.

cerebral cortex and hippocampus of Q331K mice was reduced to 60% ($p = 0.00035$) and 50% ($p = 0.0812$), respectively, of mouse TDP-43 mRNA in the nontransgenic mice (Fig. 8A). Next, we examined TDP-43 expression and subcellular localization using immunoblotting and immunofluorescence, respectively, to probe the potential pathogenic mechanisms caused by Q331K expression. Consistent with the qRT-PCR results, the human TDP-43 transgene expression is accompanied with the downregulation of the endogenous mouse TDP-43 in total homogenates of cerebral cortex and hippocampus (Fig. 8B). Furthermore, the human TDP-43 transgene expression levels are comparable between cerebral cortex and hippocampus (Fig. 8B). However, as the antibody used at this study showed a slight preference toward human TDP-43 when compared with mouse TDP-43 (Supplementary Fig. 10), we further quantified the TDP-43 protein expression with the known amount of recombinant human and mouse TDP-43 to estimate the transgene expression level (Fig. 8C). Specifically, the amount of human transgene and mouse TDP-43 from cerebral cortex of wild-type and Q331K mice were estimated based on the standard curve of known amount of recombinant human and mouse TDP-43 proteins. Human TDP-43 transgene expresses at 14.6 ± 0.7 ng per 30 μg of whole brain homogenate, whereas the endogenous TDP-43 expresses at 20.1 ± 1.0 ng. Further normalization with GAPDH suggested that human TDP-43 expressed at 22.10 ± 1.1 ng, which is comparable with the mouse TDP-43 in the wild-type mice. Taken together, the data indicate that human Q331K TDP-43 transgene expresses at the normal physiological level by, at least in part, downregulating mouse TDP-43 mRNA.

Both pathological TDP-43 aggregates and cytosolic TDP-43 accumulation are pathological hallmarks in ALS-FTD spectrum disease. Because they have been proposed as potential pathogenic mechanisms, we examined TDP-43 subcellular localization using immunofluorescence. Similar to endogenous TDP-43, Q331K TDP-43 transgene was predominantly restricted to the neuronal nuclei without apparent TDP-43 aggregates in cerebral cortex (upper panel, Fig. 8D). Furthermore, the nuclear envelope, which is labeled with lamin B, showed normal morphology and was similar with that in the nontransgenic mice (upper panel, Fig. 8D). Normal nuclear TDP-43 and normal nuclear envelop were also observed in the CA1 and dentate gyrus region of hippocampus (middle and bottom panel, Fig. 8D). These suggest that there were no apparent TDP-43 aggregates, nuclear envelope defects, and nuclear-cytosolic redistribution of TDP-43 in the cerebral cortex and hippocampus of Q331K mice.

Table 12
Means and standard deviations for distances traveled during the spatial reversal training and probe trials for the water maze

Trial type	Genotype	Gender	Age (mo)	Average (mm)	± SEM
Training	Nontg	Female	6	366	102
			12	N.A.	N.A.
		Male	6	248	67.8
			12	261	20.9
		Combined	6	303	60.0
			12	261	20.9
	Q331K	Female	6	502	46.7
			12	N.A.	N.A.
		Male	6	360	65.2
			12	374	39.4
		Combined	6	445	41.3
			12	374	39.4
Probe	Nontg	Female	6	507	70.4
			12	N.A.	N.A.
		Male	6	468	50.5
			12	850	114
		Combined	6	486	40.9
			12	850	114
	Q331K	Female	6	557	18.0
			12	N.A.	N.A.
		Male	6	560	108
			12	634	146
		Combined	6	558	42.1
			12	634	146

4. Discussion

In this study, we performed a battery of behavior tests that characterized the motor and cognitive phenotypes of Q331K mice in a longitudinal manner, with the same set of mice assessed at 3, 6, and 12 months of age. Q331K mice presented with motor deficits during early adulthood (3 months of age) and these deficits persisted through to 12 months of age. Furthermore, by systematically characterizing the cognitive phenotypes, Q331K mice showed deficits in frontal cortex–mediated working memory and cognitive flexibility, whereas their hippocampus-dependent spatial learning and memory, and contextual fear memory remained normal (Fig. 9). Biochemically, human TDP-43 downregulates mouse TDP-43 in both RNA and protein level, resulting in Q331K expression at normal physiological level in both cerebral cortex and hippocampus. Furthermore, there are no apparent TDP-43 aggregates or deformation of nuclear envelope. Taken together, the data suggest that the motor cortex and the frontal cortex may be more vulnerable to the expression of disease-linked mutation in TDP-43, which supports the notion of ALS-FTD as a disease continuum. Thus, the Q331K mice may be a suitable model to assess ALS-FTD–related spectrum diseases and the molecular underpinnings associated with the phenotypes.

Motor deficits are commonly observed in TDP-43 transgenic mouse models. These include mice overexpressing wild-type human TDP-43 under an excitatory neuron promoter (CaMK-II) (Tsai et al., 2010) or a murine prion promoter (Tsuiji et al., 2017), and BAC (bacteria artificial chromosome) transgene with ALS-linked mutations in TDP-43, such as A315T, G348C, and M337V (Gordon

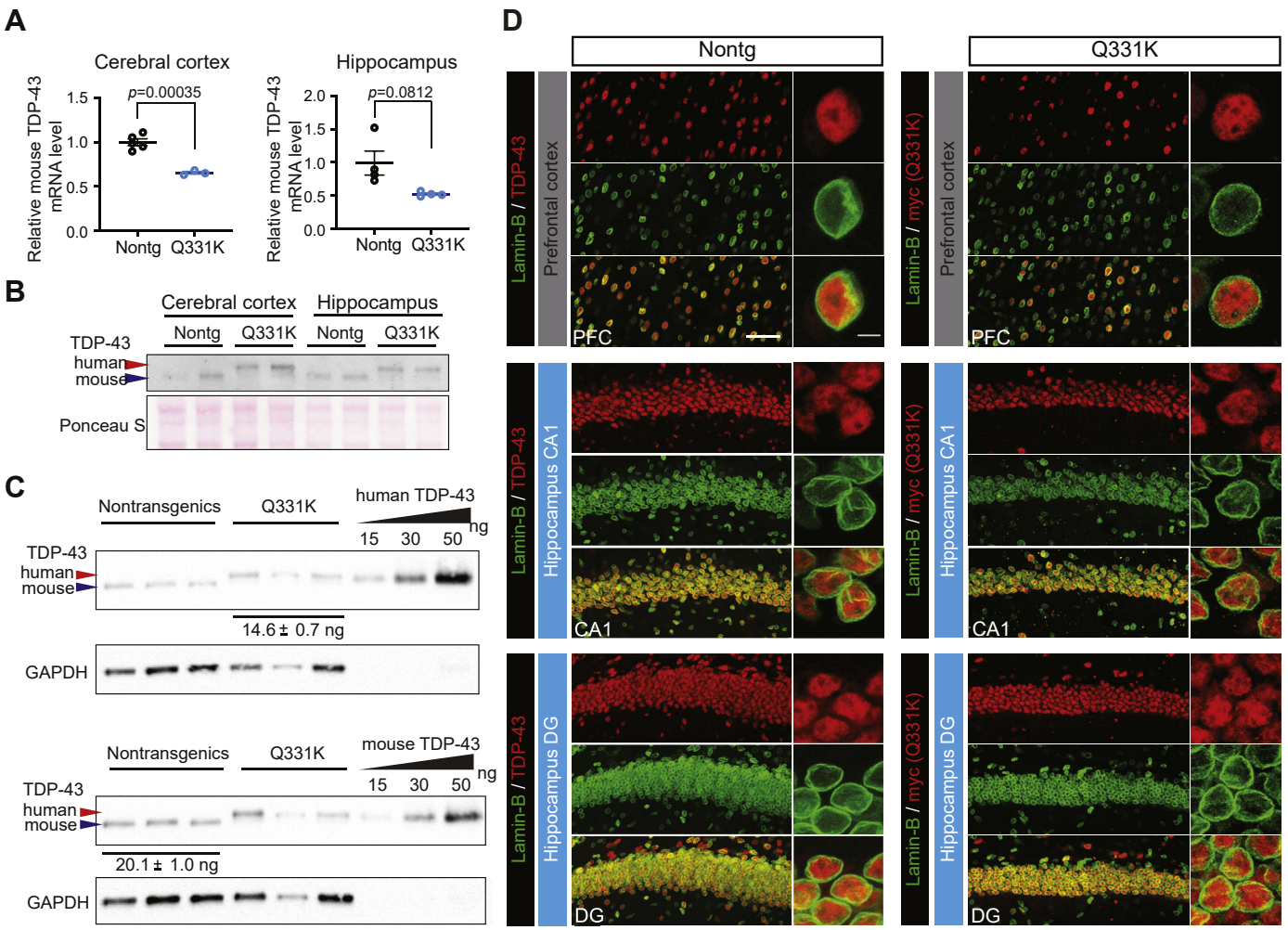

Fig. 8. Human TDP-43 transgene expresses at the comparable level as the endogenous mouse counterpart without apparent aggregates. (A) Relative mRNA expression of mouse TDP-43 in cerebral cortex and hippocampus. Expression levels of mouse TDP-43 mRNA in Q331K mice is approximately 60% and 50% to that of nontransgenic mice in cerebral cortex and hippocampus, respectively (n = 5, nontransgenic mice; n = 3, Q331K mice). (B) TDP-43 immunoblots of total homogenate from cerebral cortices and hippocampi of non-transgenic and Q331K mice. Ponceau S staining was used to examine the proper loading. n = 3, for both nontransgenic and Q331 mice. Representative blot was shown here. (C) Estimation of TDP-43 levels in the cerebral cortex of Q331K and nontransgenic mice using known amounts of recombinant human and mouse TDP-43 protein. Q331K mice express 14.6 ± 0.7 ng of human TDP-43 protein per 30 μg of total homogenate (upper panel). Nontransgenic mice express 20.1 ± 1.0 ng of endogenous TDP-43 protein per 30 μg of whole brain homogenate (lower panel). n = 3, for both nontransgenic and Q331 mice. (D) Subcellular localization of TDP-43 shows that the endogenous TDP-43 (red, in "non-tg" panel) and Q331K TDP-43 transgene (red, in "Q331K" panel) was predominantly found in the neuronal nuclei and the nuclear envelope, labeled with lamin B (green), showed similar morphologies to nontransgenic mice across prefrontal cortex (PFC, upper panel), CA1 region of hippocampus (CA1, middle panel) and dentate gyrus (DG) region of hippocampus (DG, lower panel). n = 3, for both non-transgenic and Q331 mice. Scale bar is 50 μm and 5 μm, respectively. (For interpretation of the references to color in this figure legend, the reader is referred to the Web version of this article.)

et al., 2019; Swarup et al., 2011). Here, 2 assays were used to assess motor phenotypes: (1) the rotarod, which assessed gross motor coordination (McAleese et al., 2017; Uchino et al., 2015), and (2) the balance beam, which assessed fine motor coordination and balance (Luong et al., 2011; Tung et al., 2016). Our results are in congruence with previous studies (Arnold et al., 2013; Ditsworth et al., 2017), showing that Q331K mice performed poorly on both motor tests compared with nontransgenic mice starting from 3 months of age and that the motor coordination deficit persisted through to 6 and 12 months of age. In addition, the Q331K mice were slower to improve in their abilities in both motor coordination tests than nontransgenic mice with an increasing number of training days. Furthermore, as the same set of animals were tested across 3 time points in this study, nontransgenic mice showed more carry-over learning or rapid relearning from the previous testing time points compared with Q331K mice. This is more obvious in the balance beam test, when at the 6- and 12-month time points, nontransgenic mice started their first training sessions at a lower latency than the corresponding training session at 3 months of age. By contrast, Q331K mice showed similar starting latencies for their first training session at each testing time point. These observations suggest that as Q331K mice age, the early motor deficits that were exhibited may be compounded by poorer motor coordination learning due to cognitive perturbations (see the following).

Similar to motor deficits, Q331K mice, from 3 months of age, developed long-lasting cognitive deficits in working memory, STM, and cognitive flexibility tasks that involve the frontal cortex (Boulougouris et al., 2007; McDonald and White, 1994; Rich and Shapiro, 2007; Tsutsui et al., 2016). By contrast, Q331K mice performed comparably with nontransgenic mice in hippocampus-dependent tasks, suggesting relatively intact hippocampal functions. This is consistent with patient studies, where deficits in executive dysfunctions, language, social cognition, and disinhibition observed in FTLD-TDP (FTD with TDP-43 pathology) patients

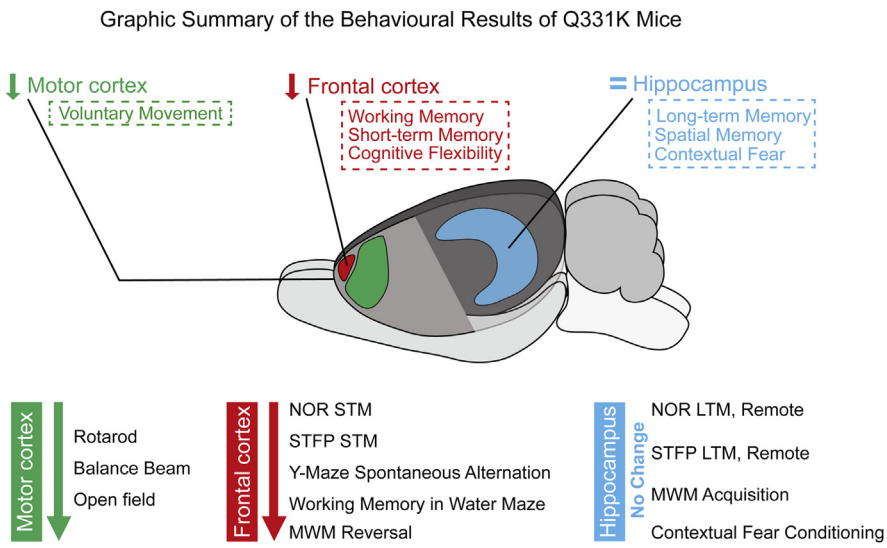

Fig. 9. A summary diagram of the findings from the battery of behavioral assays that were run on Q331K mice and their nontransgenic counterparts. Our findings suggest that Q331K mice developed motor deficit phenotypes from 3 months of age and these persisted through to 12 months of age. In addition, Q331K mice also developed persistent frontal cortex–mediated behavioral deficits from an early age. Last but not least, Q331K mice did not seem to develop hippocampus-mediated behavioral deficits compared with nontransgenic controls.

(Guedes et al., 2017) and cognitive impairments in patients with ALS (Strong et al., 2017) are attributed to the degeneration of prefrontal cortex (Abrahams et al., 2005; Canosa et al., 2016; Schuster et al., 2014; Turner et al., 2012). Furthermore, Q331K knock-in mice also have executive function deficits (White et al., 2018), further suggesting that their frontal cortex functions were compromised due to TDP-43 mutation. By contrast, TDP-43 mouse models with an overexpression of wild-type mouse (Tsai et al., 2010) and human (Swarup et al., 2011; Tsuiji et al., 2017) TDP-43 showed hippocampus-mediated cognitive deficits. For example, CaMK-II promoter driven wild-type mouse TDP-43 (Tsai et al., 2010) and prion-promoter driven wild-type human TDP-43 transgene (Tsuiji et al., 2017) showed deficits in water maze and fear conditioning tasks, but not in the Y maze task (Tsuiji et al., 2017). Transgenic mice expressing BAC containing wild type and G348C mutation in human TDP-43 showed deficits in Barnes maze (Swarup et al., 2011), which also a hippocampus-mediated cognitive task. By contrast, our Q331K mice performed at similar levels to nontransgenic mice during the LTM and RM probes in the Morris water maze and contextual fear conditioning tests. The data suggest that the consolidation and retrieval functions of the hippocampus and anterior cingulate of Q331K mice were not affected (Ben-Yakov et al., 2015; Bontempi et al., 1999; Frankland and Bontempi, 2005; Frankland et al., 2004). Thus, comparing and contrasting the expression profiling, such as RNA-seq, within the frontal cortex and hippocampus may provide potential molecular mechanisms underlying TDP-43 mediated neurotoxicity.

Elevated TDP-43 level is sufficient to induce neuronal toxicity (Mitchell et al., 2015; Wils et al., 2010), which often confounds the interpretation of data obtaining from transgenic animals. Using known amount of recombinant human and mouse TDP-43, we were able to establish that the human Q331K transgene expresses comparably with the physiological TDP-43 level in mice. Furthermore, human Q331K transgene downregulates the endogenous mouse TDP-43 protein by, at least in part, reducing the TDP-43 mRNA level. Human Q331K transgene also shows normal nuclear localization without apparently aggregates or nuclear envelope deficits. Finally, cerebral cortex and hippocampus has comparable Q331K expression. Thus, the phenotypes of the mice are likely caused by the expression of disease-linked mutation in TDP-43, rather than the levels. As Q331K mice developed early and persistent deficits in motor functions and frontal cortex–mediated tasks, our data suggest that the motor cortex and the frontal cortex may be more vulnerable to the expression of disease-linked mutations in TDP-43. Taken together, the results of our systematic behavioral assessment provide a framework to further use this mouse model for investigating the pathophysiology and the molecular underpinnings of the ALS-FTD spectrum disease.

Disclosure statement

The authors declare that they have no conflict of interest.

CRediT authorship contribution statement

Peiyan Wong: Conceptualization, Methodology, Validation, Formal analysis, Investigation, Data curation, Writing - original draft, Writing - review & editing, Visualization, Supervision. **Wan Yun Ho:** Methodology, Validation, Formal analysis, Investigation, Resources, Data curation, Visualization, Project administration. **Yi-Chun Yen:** Methodology, Validation, Formal analysis, Investigation. **Emma Sanford:** Methodology, Validation, Formal analysis, Investigation, Writing - review & editing. **Shuo-Chien Ling:** Conceptualization, Methodology, Validation, Formal analysis, Investigation, Resources, Data curation, Writing - original draft, Writing - review & editing, Visualization, Supervision, Project administration, Funding acquisition.

Acknowledgements

The authors thank all of the Ling laboratory members for support, discussion, and suggestions. The behavioral experiments were carried out at the Neuroscience Phenotyping Core Facility, which is supported by the NMRC NUHS Centre Grant—Neuroscience Phenotyping Core (NMRC/CG/M009/2017_NUH/NUHS). This work was supported by grants to S.-C. L. from the Swee Liew-Wadsworth Endowment fund, National University of Singapore, National Medical Research Council (NMRC/OFIRG/0001/2016 and NMRC/OFIRG/0042/2017), and the Ministry of Education (MOE2016-T2-1-

024), Singapore. S.-C. Ling. dedicates this work to the memory of Sheue-Houy Tyan.

Appendix A. Supplementary data

Supplementary data associated with this article can be found, in the online version, at https://doi.org/10.1016/j.neurobiolaging.2020.03.019.

References

Abrahams, S., Goldstein, L.H., Suckling, J., Ng, V., Simmons, A., Chitnis, X., Atkins, L., Williams, S.C.R., Leigh, P.N., 2005. Frontotemporal white matter changes in amyotrophic lateral sclerosis. J. Neurol. 252, 321–331.

Amador-Ortiz, C., Lin, W.-L., Ahmed, Z., Personett, D., Davies, P., Duara, R., Graff-Radford, N.R., Hutton, M.L., Dickson, D.W., 2007. TDP-43 immunoreactivity in hippocampal sclerosis and Alzheimer's disease. Ann. Neurol. 61, 435–445.

Aoki, N., Murray, M.E., Ogaki, K., Fujioka, S., Rutherford, N.J., Rademakers, R., Ross, O.A., Dickson, D.W., 2015. Hippocampal sclerosis in Lewy body disease is a TDP-43 proteinopathy similar to FTLD-TDP Type A. Acta Neuropathol. (Berl.) 129, 53–64.

Arai, T., Hasegawa, M., Akiyama, H., Ikeda, K., Nonaka, T., Mori, H., Mann, D., Tsuchiya, K., Yoshida, M., Hashizume, Y., Oda, T., 2006. TDP-43 is a component of ubiquitin-positive tau-negative inclusions in frontotemporal lobar degeneration and amyotrophic lateral sclerosis. Biochem. Biophys. Res. Commun. 351, 602–611.

Arnold, E.S., Ling, S.-C., Huelga, S.C., Lagier-Tourenne, C., Polymenidou, M., Ditsworth, D., Kordasiewicz, H.B., McAlonis-Downes, M., Platoshyn, O., Parone, P.A., Da Cruz, S., Clutario, K.M., Swing, D., Tessarollo, L., Marsala, M., Shaw, C.E., Yeo, G.W., Cleveland, D.W., 2013. ALS-linked TDP-43 mutations produce aberrant RNA splicing and adult-onset motor neuron disease without aggregation or loss of nuclear TDP-43. Proc. Natl. Acad. Sci. U. S. A. 110, E736–E745.

Bates, D., Mächler, M., Bolker, B., Walker, S., 2015. Fitting linear mixed-effects models using lme4. J. Stat. Softw. 67, 1–48.

Ben-Yakov, A., Dudai, Y., Mayford, M.R., 2015. Memory retrieval in mice and men. Cold Spring Harb. Perspect. Biol. a021790.

Bertram, L., Tanzi, R.E., 2005. The genetic epidemiology of neurodegenerative disease. J. Clin. Invest. 115, 1449–1457.

Bontempi, B., Laurent-Demir, C., Destrade, C., Jaffard, R., 1999. Time-dependent reorganization of brain circuitry underlying long-term memory storage. Nature 400, 671–675.

Boulougouris, V., Dalley, J.W., Robbins, T.W., 2007. Effects of orbitofrontal, infralimbic and prelimbic cortical lesions on serial spatial reversal learning in the rat. Behav. Brain Res. 179, 219–228.

Brettschneider, J., Del Tredici, K., Lee, V.M.-Y., Trojanowski, J.Q., 2015. Spreading of pathology in neurodegenerative diseases: a focus on human studies. Nat. Rev. Neurosci. 16, 109–120.

Brettschneider, J., Libon, D.J., Toledo, J.B., Xie, S.X., McCluskey, L., Elman, L., Geser, F., Lee, V.M.-Y., Grossman, M., Trojanowski, J.Q., 2012. Microglial activation and TDP-43 pathology correlate with executive dysfunction in amyotrophic lateral sclerosis. Acta Neuropathol. (Berl.) 123, 395–407.

Burgess, N., Maguire, E.A., O'Keefe, J., 2002. The human hippocampus and spatial and episodic memory. Neuron 35, 625–641.

Canosa, A., Pagani, M., Cistaro, A., Montuschi, A., Iazzolino, B., Fania, P., Cammarosano, S., Ilardi, A., Moglia, C., Calvo, A., Chiò, A., 2016. F-FDG-PET correlates of cognitive impairment in ALS. Neurology 86, 44.

Ditsworth, D., Maldonado, M., McAlonis-Downes, M., Sun, S., Seelman, A., Drenner, K., Arnold, E., Ling, S.-C., Pizzo, D., Ravits, J., Cleveland, D.W., Da Cruz, S., 2017. Mutant TDP-43 within motor neurons drives disease onset but not progression in amyotrophic lateral sclerosis. Acta Neuropathol. (Berl.) 133, 907–922.

Ebstein, S.Y., Yagudayeva, I., Shneider, N.A., 2019. Mutant TDP-43 causes early-stage dose-dependent motor neuron degeneration in a TARDBP Knockin mouse model of ALS. Cell Rep 26, 364–373.e4.

Eichenbaum, H., 2004. Hippocampus: cognitive processes and neural representations that underlie declarative memory. Neuron 44, 109–120.

Foster, T.C., DeFazio, R.A., Bizon, J.L., 2012. Characterizing cognitive aging of spatial and contextual memory in animal models. Front. Aging Neurosci. 4, 12.

Frankland, P.W., Bontempi, B., 2005. The organization of recent and remote memories. Nat. Rev. Neurosci. 6, 119–130.

Frankland, P.W., Bontempi, B., Talton, L.E., Kaczmarek, L., Silva, A.J., 2004. The involvement of the anterior cingulate cortex in remote contextual fear memory. Science 304, 881–883.

Franklin, K.B.J., Chudasama, Y., 2012. Chapter 30 - prefrontal cortex. In: Watson, C., Paxinos, G., Puelles, L. (Eds.), The Mouse Nervous System. Academic Press, San Diego, pp. 727–735.

Fuster, J.M., 2001. Prefrontal cortex. In: Smelser, N.J., Baltes, P.B. (Eds.), International Encyclopedia of the Social & Behavioral Sciences. Pergamon, Oxford, pp. 11969–11976.

Gordon, D., Dafinca, R., Scaber, J., Alegre-Abarrategui, J., Farrimond, L., Scott, C., Biggs, D., Kent, L., Oliver, P.L., Davies, B., Ansorge, O., Wade-Martins, R., Talbot, K., 2019. Single-copy expression of an amyotrophic lateral sclerosis-linked TDP-43 mutation (M337V) in BAC transgenic mice leads to altered stress granule dynamics and progressive motor dysfunction. Neurobiol. Dis. 121, 148–162.

Guedes, Á.C.B., Santin, R., Costa, A.S.R., Reiter, K.C., Hilbig, A., Fernandez, L.L., 2017. Distinct Phospho-TDP-43 brain distribution in two cases of FTD, one associated with ALS. Dement. Neuropsychol. 11, 249–254.

Ho, W.Y., Chang, J.-C., Tyan, S.-H., Yen, Y.-C., Lim, K., Tan, B.S.Y., Ong, J., Tucker-Kellogg, G., Wong, P., Koo, E., Ling, S.-C., 2019. FUS-mediated dysregulation of Sema5a, an autism-related gene, in FUS mice with hippocampus-dependent cognitive deficits. Hum. Mol. Genet. 28, 3777–3791.

Josephs, K.A., Murray, M.E., Whitwell, J.L., Parisi, J.E., Petrucelli, L., Jack, C.R., Petersen, R.C., Dickson, D.W., 2014. Staging TDP-43 pathology in Alzheimer's disease. Acta Neuropathol. (Berl.) 127, 441–450.

Kim, C., Johnson, N.F., Cilles, S.E., Gold, B.T., 2011. Common and distinct mechanisms of cognitive flexibility in prefrontal cortex. J. Neurosci. 31, 4771–4779.

Kuznetsova, A., Brockhoff, P.B., Christensen, R.H.B., 2017. **lmerTest** package: tests in linear mixed effects models. J. Stat. Softw. 82, 1–26.

Lattante, S., Rouleau, G.A., Kabashi, E., 2013. TARDBP and FUS mutations associated with amyotrophic lateral sclerosis: summary and Update. Hum. Mutat. 34, 812–826.

Ling, S.-C., 2018. Synaptic Paths to neurodegeneration: the emerging role of TDP-43 and FUS in synaptic functions. Neural Plast. 2018, 8413496.

Ling, S.-C., Albuquerque, C.P., Han, J.S., Lagier-Tourenne, C., Tokunaga, S., Zhou, H., Cleveland, D.W., 2010. ALS-associated mutations in TDP-43 increase its stability and promote TDP-43 complexes with FUS/TLS. Proc. Natl. Acad. Sci. U. S. A. 107, 13318–13323.

Ling, S.-C., Polymenidou, M., Cleveland, D.W., 2013. Converging mechanisms in ALS and FTD: disrupted RNA and protein homeostasis. Neuron 79, 416–438.

Luong, T.N., Carlisle, H.J., Southwell, A., Patterson, P.H., 2011. Assessment of motor balance and coordination in mice using the balance beam. J. Vis. Exp. Jove.

McAleese, K.E., Walker, L., Graham, S., Moya, E.L.J., Johnson, M., Erskine, D., Colloby, S.J., Dey, M., Martin-Ruiz, C., Taylor, J.-P., Thomas, A.J., McKeith, I.G., De Carli, C., Attems, J., 2017. Parietal white matter lesions in Alzheimer's disease are associated with cortical neurodegenerative pathology, but not with small vessel disease. Acta Neuropathol. (Berl.) 134, 459–473.

McDonald, R.J., White, N.M., 1994. Parallel information processing in the water maze: evidence for independent memory systems involving dorsal striatum and hippocampus. Behav. Neural Biol. 61, 260–270.

Mitchell, J.C., Constable, R., So, E., Vance, C., Scotter, E., Glover, L., Hortobágyi, T., Arnold, E.S., Ling, S.-C., McAlonis, M., Da Cruz, S., Polymenidou, M., Tessarolo, L., Cleveland, D.W., Shaw, C.E., 2015. Wild type human TDP-43 potentiates ALS-linked mutant TDP-43 driven progressive motor and cortical neuron degeneration with pathological features of ALS. Acta Neuropathol. Commun. 3, 36.

Nag, S., Yu, L., Boyle, P.A., Leurgans, S.E., Bennett, D.A., Schneider, J.A., 2018. TDP-43 pathology in anterior temporal pole cortex in aging and Alzheimer's disease. Acta Neuropathol. Commun. 6, 33.

Nag, S., Yu, L., Capuano, A.W., Wilson, R.S., Leurgans, S.E., Bennett, D.A., Schneider, J.A., 2015. Hippocampal sclerosis and TDP-43 pathology in aging and Alzheimer's Disease. Ann. Neurol. 77, 942–952.

Nelson, P.T., Dickson, D.W., Trojanowski, J.Q., Jack, C.R., Boyle, P.A., Arfanakis, K., Rademakers, R., Alafuzoff, I., Attems, J., Brayne, C., Coyle-Gilchrist, I.T.S., Chui, H.C., Fardo, D.W., Flanagan, M.E., Halliday, G., Hokkanen, S.R.K., Hunter, S., Jicha, G.A., Katsumata, Y., Kawas, C.H., Keene, C.D., Kovacs, G.G., Kukull, W.A., Levey, A.I., Makkinejad, N., Montine, T.J., Murayama, S., Murray, M.E., Nag, S., Rissman, R.A., Seeley, W.W., Sperling, R.A., White III, C.L., Yu, L., Schneider, J.A., 2019. Limbic-predominant age-related TDP-43 encephalopathy (LATE): consensus working group report. Brain 142, 1503–1527.

Neumann, M., Sampathu, D.M., Kwong, L.K., Truax, A.C., Micsenyi, M.C., Chou, T.T., Bruce, J., Schuck, T., Grossman, M., Clark, C.M., McCluskey, L.F., Miller, B.L., Masliah, E., Mackenzie, I.R., Feldman, H., Feiden, W., Kretzschmar, H.A., Trojanowski, J.Q., Lee, V.M.-Y., 2006. Ubiquitinated TDP-43 in frontotemporal lobar degeneration and amyotrophic lateral sclerosis. Science 314, 130–133.

Polymenidou, M., Lagier-Tourenne, C., Hutt, K.R., Huelga, S.C., Moran, J., Liang, T.Y., Ling, S.-C., Sun, E., Wancewicz, E., Mazur, C., Kordasiewicz, H., Sedaghat, Y., Donohue, J.P., Shiue, L., Bennett, C.F., Yeo, G.W., Cleveland, D.W., 2011. Long pre-mRNA depletion and RNA missplicing contribute to neuronal vulnerability from loss of TDP-43. Nat. Neurosci. 14, 459–468.

Rich, E.L., Shapiro, M.L., 2007. Prelimbic/Infralimbic inactivation impairs memory for multiple task switches, but not flexible selection of familiar tasks. J. Neurosci. 27, 4747–4755.

Rohrer, J.D., Geser, F., Zhou, J., Gennatas, E.D., Sidhu, M., Trojanowski, J.Q., DeArmond, S.J., Miller, B.L., Seeley, W.W., 2010. TDP-43 subtypes are associated with distinct atrophy patterns in frontotemporal dementia. Neurology 75, 2204.

Schuster, C., Kasper, E., Dyrba, M., Machts, J., Bittner, D., Kaufmann, J., Mitchell, A.J., Benecke, R., Teipel, S., Vielhaber, S., Prudlo, J., 2014. Cortical thinning and its relation to cognition in amyotrophic lateral sclerosis. Neurobiol. Aging 35, 240–246.

Strong, M.J., Abrahams, S., Goldstein, L.H., Woolley, S., Mclaughlin, P., Snowden, J., Mioshi, E., Roberts-South, A., Benatar, M., HortobáGyi, T., Rosenfeld, J., Silani, V., Ince, P.G., Turner, M.R., 2017. Amyotrophic lateral sclerosis - frontotemporal spectrum disorder (ALS-FTSD): revised diagnostic criteria. Amyotroph. Lateral Scler. Front. Degener. 18, 153–174.

Swarup, V., Phaneuf, D., Bareil, C., Robertson, J., Rouleau, G.A., Kriz, J., Julien, J.-P., 2011. Pathological hallmarks of amyotrophic lateral sclerosis/frontotemporal lobar degeneration in transgenic mice produced with TDP-43 genomic fragments. Brain 134, 1–17.

Tsai, K.-J., Yang, C.-H., Fang, Y.-H., Cho, K.-H., Chien, W.-L., Wang, W.-T., Wu, T.-W., Lin, C.-P., Fu, W.-M., Shen, C.-K.J., 2010. Elevated expression of TDP-43 in the forebrain of mice is sufficient to cause neurological and pathological phenotypes mimicking FTLD-U. J. Exp. Med. 207, 1661–1673.

Tsermentseli, S., Leigh, P.N., Goldstein, L.H., 2012. The anatomy of cognitive impairment in amyotrophic lateral sclerosis: more than frontal lobe dysfunction. Cortex 48, 166–182.

Tsuiji, H., Inoue, I., Takeuchi, M., Furuya, A., Yamakage, Y., Watanabe, S., Koike, M., Hattori, M., Yamanaka, K., 2017. TDP-43 accelerates age-dependent degeneration of interneurons. Sci. Rep. 7, 14972.

Tsutsui, K.-I., Oyama, K., Nakamura, S., Iijima, T., 2016. Comparative overview of visuospatial working memory in monkeys and rats. Front. Syst. Neurosci. 10, 99.

Tung, V.W.K., Burton, T.J., Quail, S.L., Mathews, M.A., Camp, A.J., 2016. Motor performance is impaired following vestibular stimulation in ageing mice. Front. Aging Neurosci. 8, 12.

Turner, M.R., Agosta, F., Bede, P., Govind, V., Lulé, D., Verstraete, E., 2012. Neuroimaging in amyotrophic lateral sclerosis. Biomark. Med. 6, 319–337.

Uchino, A., Takao, M., Hatsuta, H., Sumikura, H., Nakano, Y., Nogami, A., Saito, Y., Arai, T., Nishiyama, K., Murayama, S., 2015. Incidence and extent of TDP-43 accumulation in aging human brain. Acta Neuropathol. Commun. 3, 35.

Vorhees, C.V., Williams, M.T., 2006. Morris water maze: procedures for assessing spatial and related forms of learning and memory. Nat. Protoc. 1, 848–858.

Wang, J., Ho, W.Y., Lim, K., Feng, J., Tucker-Kellogg, G., Nave, K.-A., Ling, S.-C., 2018. Cell-autonomous requirement of TDP-43, an ALS/FTD signature protein, for oligodendrocyte survival and myelination. Proc. Natl. Acad. Sci. U. S. A. 115, E10941–E10950.

Wegorzewska, I., Bell, S., Cairns, N.J., Miller, T.M., Baloh, R.H., 2009. TDP-43 mutant transgenic mice develop features of ALS and frontotemporal lobar degeneration. Proc. Natl. Acad. Sci. U. S. A. 106, 18809–18814.

White, M.A., Kim, E., Duffy, A., Adalbert, R., Phillips, B.U., Peters, O.M., Stephenson, J., Yang, S., Massenzio, F., Lin, Z., Andrews, S., Segonds-Pichon, A., Metterville, J., Saksida, L.M., Mead, R., Ribchester, R.R., Barhomi, Y., Serre, T., Coleman, M.P., Fallon, J.R., Bussey, T.J., Brown, R.H., Sreedharan, J., 2018. TDP-43 gains function due to perturbed autoregulation in a Tardbp knock-in mouse model of ALS-FTD. Nat. Neurosci. 21, 552–563.

Wils, H., Kleinberger, G., Janssens, J., Pereson, S., Joris, G., Cuijt, I., Smits, V., Ceuterick-De Groote, C., Van Broeckhoven, C., Kumar-Singh, S., 2010. TDP-43 transgenic mice develop spastic paralysis andneuronal inclusions characteristic of ALS andfrontotemporal lobar degeneration. Proc. Natl. Acad. Sci. U. S. A. 107, 1–13.

Wong, P., Sze, Y., Chang, C.C.R., Lee, J., Zhang, X., 2015. Pregnenolone sulfate normalizes schizophrenia-like behaviors in dopamine transporter knockout mice through the AKT/GSK3β pathway. Transl. Psychiatr. 5, e528.